



HAL
open science

Green polymers filaments for 3D-printing

Amélie Tribot, Dan Batalu, Clément Brasselet, Cédric Delattre, Lu Wei,
Jonathan Lao, Petre Badica, Philippe Michaud, Hélène de Baynast

► **To cite this version:**

Amélie Tribot, Dan Batalu, Clément Brasselet, Cédric Delattre, Lu Wei, et al.. Green polymers filaments for 3D-printing. Green Sustainable Process for Chemical and Environmental Engineering and Science, Elsevier, pp.463-516, 2022, 10.1016/B978-0-323-99643-3.00015-2 . hal-04056773

HAL Id: hal-04056773

<https://hal.science/hal-04056773>

Submitted on 3 Apr 2023

HAL is a multi-disciplinary open access archive for the deposit and dissemination of scientific research documents, whether they are published or not. The documents may come from teaching and research institutions in France or abroad, or from public or private research centers.

L'archive ouverte pluridisciplinaire **HAL**, est destinée au dépôt et à la diffusion de documents scientifiques de niveau recherche, publiés ou non, émanant des établissements d'enseignement et de recherche français ou étrangers, des laboratoires publics ou privés.

Green polymers filaments for 3D-printing

Amélie Tribot, Dan Batalu, Clément Brasselet, Cédric Delattre, Lu Wei, Jonathan Lao, Petre Badica, Philippe Michaud, Hélène de Baynast*

Contents

1	Introduction.....	2
2	3D printing technology.....	4
2.1	Short history of 3D printing technology.....	4
2.2	Principle of the fused deposition modeling.....	5
2.3	Production of filaments: technical approach, present status and future directions..	8

*

A. Tribot, C. Brasselet, C. Delattre, P. Michaud (✉), H. de Baynast (✉),
Université Clermont Auvergne, CNRS, SIGMA Clermont, Institut Pascal, 4 Avenue Blaise Pascal, 63178 Aubière,
amelie.tribot@uca.fr; <https://orcid.org/0000-0002-2475-5964>
clement.brasselet@uca.fr; <https://orcid.org/0000-0003-1136-6756>
cedric.delattre@uca.fr; <https://orcid.org/0000-0003-3605-1929>
philippe.michaud@uca.fr; <https://orcid.org/0000-0002-6677-4549>
helene.de_baynast@uca.fr; <https://orcid.org/0000-0001-5404-2909>

D. Batalu

University Politehnica of Bucharest, Materials Science and Engineering Faculty, Splaiul Independentei 313, Bucharest 060042, Romania
dan.batalu@upb.ro; <https://orcid.org/0000-0001-7393-5286>

J. Lao

Université Clermont Auvergne, CNRS/IN2P3, LPC, F-63000 CLERMONT-FERRAND, France
jonathan.lao@clermont.in2p3.fr

P. Badica

National Institute of Materials Physics, Atomistilor 405 A, Magurele 077125, Romania,
badica2003@yahoo.com; <https://orcid.org/0000-0003-3038-2110>

Lu Wei

Tongji University, School of Materials Science and Engineering, Shanghai Key Laboratory D&A Metallic Functional Materials, No. 4800, Cao'an Road, Shanghai [201804](#), China
weilu@tongji.edu.cn; <https://orcid.org/0000-0001-8214-7580>

2.4	Control parameters for high quality printing	11
3	Green Polymers	13
3.1	Polymers from petrochemical synthesis (group 4): Polycaprolactone (PCL)	14
3.2	Polymers from biotechnology (group 3)	19
3.2.1	Poly(lactic acid) (PLA).....	19
3.2.2	Butanediol Polyesters.....	25
3.2.3.	Polybutyrate adipate terephthalate (PBAT).....	28
3-3	Polymers from microorganisms obtained by extraction (group 2): Polyhydroxyalcanoates (PHA)	29
3-4	Polymers from biomass (group 1)	32
3.4.1	Starch (TPS).....	32
3.4.2	Cellulose	35
3.4.3	Lignin	36
3.4.4	Chitosan.....	41
4	Conclusion	42
	References.....	43

Abstract

3D printing or additive manufacturing is a technology that has drastically developed in recent years for numerous industrial applications. Among the 3D printing methods the fused deposition modeling (requires filaments to generate a three dimensional objects. Currently, the polymers used in this technology are synthetic ones, derived from non renewable resources such as petroleum. Green polymers (including natural polymers) are a sustainable alternative of them as they are biodegradable/recyclable, non toxic and abundant. However the implementation in 3D printing of the major part of them remains a challenge. This chapter is focused on the most famous and promising biodegradable polymers from biomass, produced by microorganisms or derived from biotechnology for applications using fused deposition modeling. Their thermal, rheological and mechanical properties are also discussed in details.

Keywords

Biopolymer, green polymer, 3D-printing, Fused deposition modeling

1 Introduction

Synthetic polymers have become indispensable to our daily life. They are at the basis of a large range of modern applications including materials, packaging consumer's products, food and other. Their commercial and technical success emerged during the second part of the 20th century. It was based on their low costs but above all on their resistance to chemical,

physical and biological degradations. This success is today at the origin of researches for green polymers as an alternative to synthetic ones to satisfy the conditions of biodegradability, low-toxicity (including that of degradation products) and sustainability. Indeed, the resistance of synthetic polymers to degradation and their mass consumption produce more and more resistant wastes becoming less and less acceptable. What is a green polymer? According to the International Union of Pure and Applied Chemistry (<https://iupac.org/>), green polymers are manufactured by the green chemistry, green chemistry relating to the “design of chemical products and processes that reduce or eliminate the use or generation of hazardous substances for animals, plants and environment”. The main characteristic of green polymers is their biodegradability which can be defined as a degradation occurring through the action of enzymes and /or biochemical compounds produced by living microorganisms. It is often associated with abiotic degradation due to natural environment (oxidation or photodegradation for examples). This biodegradation leads to the formation of H₂O, CO₂, CH₄ and low molecular weight products. Natural polymers or biopolymers such as nucleic acids, proteins or polysaccharides are usually green. So in this chapter natural polymers will be design as green polymers. Biopolymers are abundant in nature and diverse in respect of their structures. They exhibit a wide range of properties depending on their biological functions. At this time, biochemists divide biopolymers into 8 major classes: polyphenols such as humic acids or lignins, polyisoprenoids, inorganic polyesters (polyphosphate), polythioesters, cutin and polymalic acid, polyoxoesters, polysaccharides, polyamides and nucleic acids. They are abundant, sustainable and eco-friendly polymers. They have chemical groups, compatible with chemical modifications. However, these biopolymers have low printing performances and this issue has to be overcome for production of 3D object at large scale.

3D printing also known as additive manufacturing has drastically developed in recent years. Additive manufacturing can produce everything such as food, clothes, bikes, cars, washing machines or houses. The process includes constructing a 3D object through a successive layer-by-layer depositions of materials under a computer control. The two early 3D-printing methods have been invented by Kodama of the Nagoya Municipal Industrial Research Institute, to manufacture 3D plastic materials in 1981 using a photosensitive polymer (Kodama, 1981). The term 3D-printing designs polymer technologies whereas that of additive manufacturing was used in metal working. The materials used are various: plastic, metal, ceramic, living cells or food. There exist few 3D printing methods: Fused Deposition Modeling (FDM), direct ink printing, continuous or drop-on-demand inkjet printing, Electron Beam Direct manufacturing, Stereolithography (SLA), Selective Laser Sintering (SLS), depending of the material and the application researched (Liu et al., 2019).

This chapter will be restricted to the Fused Deposition Modeling technology. It will be treated only of the manufacturing and the implementation of biodegradable green polymers through their printability. It will be focused on their thermal, rheological and mechanical properties.

2 3D printing technology

2.1 Short history of 3D printing technology

3D printing technology appeared at the right moment, because of the inspiration of the inventor and the development of the computer assisted design and manufacturing (CAD and CAM, respectively). It was probably the next natural step to integrate previous technologies into one programmable machine, that can fabricate 3D objects with high reproducibility and accuracy. For a better understanding of this “natural” step forward we present the following short timeline of the inventions that led to Fused Deposition Modelling (FDM) technology.

In 1936 was published the patent entitled “Soldering iron” by Henry Joseph Leitsch, describing an electric device used for soldering (Leitsch, 1936). The principle of feeding the soldering alloy through a tube with a hot area inspired the invention of the hot glue gun. In 1938, a similar device, but using wax for sealing was patented by John Pesark (1938). The patent was called “Device for applying sealing wax”. In 1951, the patent “Plastic welding device” of Richard Smurthwaite Arkless (1951), introduced the idea of using thermo-plastic materials for welding.

In 1965 was issued the patent “Portable thermoplastic cement dispenser” , a precursor of the current (hot) glue gun, where we can find very similar elements with the extruder head of a 3D printer, and of the later 3D pen (Paulsen, 1965). It was designed to use thermoplastic filaments. In 1986 was introduced the 3D printing concept by stereolithography, through the patent “Apparatus for production of three-dimensional objects by stereolithography” (Hull, 1986). The patent claimed obtaining 3D objects from liquid resins by solidifying selected areas, layer by layer, using various sources depending on materials (X-ray, ultraviolet light, an electron beam, laser, a jet of reactive chemical, etc). However, it is worthy to mention here the scientific paper of Hideo Kodama, published 5 years earlier on a similar topic, where he proposed ultraviolet light guided through an optical fiber for hardening a polymer into a 3D shape (Kodama, 1981). Other even earlier patents, not mentioned here, refer to 3D images using photopolymerization.

In 1987 the STL file format was developed for 3D Systems, and it is still in use as a main format to communicate with 3D printers. In 1992 was published the patent entitled “Apparatus and methods for creating three-dimensional objects”, assigned to Stratasys Inc, where the inventor is Steven Scott Crump (1989). The patent was filed in October 30, 1989, and the story tells that the idea came out when the inventor created a toy for his daughter using a glue gun. Anyhow, as we can see from the evolution of 3D printing, the main merit is introduction in use of thermoplastics for 3D printing. The technology is known today as Fused Filament Fabrication (FFF, name proposed by RepRap community project) or Fused Deposition Modeling (FDM, Stratasys trademark name).

An important change in the status of FDM happened when the patent of the technology expired in 2009 October 30. Since then a real explosion of 3D printer companies and DIY (Do It Yourself) projects occurred, as the electronics and mechanical components (inexpensive, reliable, and easy to use microcontrollers, sensors, motors, and other components) became easily available.

Also, the enthusiasm of hobbyists made the FDM 3D printers very accessible, and their improvement is continuing, sometimes surpassing the commercial technology. Some future directions of 3D printing technology are related to:

- (i) increase the equipment's accuracy, speed, resolution, temperature and materials range;
- (ii) creation of new functional materials for FDM that can provide ready to use and smart objects;
- (iii) development of more advanced software for 3D printing;
- (iv) recycling aspects, making 3D printing a green technology.

Based on classification proposed in ISO/ASTM 52900:2015, new directions can be envisioned for improving or developing new ceramics, metals, polymers, and composites (ISO/ASTM 52900, 2015, p. 1-9.). Currently, new technologies are already on the market or proposed, such as 3D bioprinting, polyjet 3D printing, rapid liquid printing (using gel suspension), two-photon polymerization 3D printing (working at micro/nanoscale). Future development of new materials and technologies will surely go beyond the limits of what we know or imagine today.

2.2 Principle of the fused deposition modeling

Looking at the evolution of FDM, the main idea is to use a programmable machine (additive manufacturing machine (ISO/ASTM 52900, 2015, p. 1-9.) that will deposit, following a certain pattern, a melted polymer on a build platform and will continue adding layers on previous ones. The melted state of the polymer is necessary both for easily changing the filament shape along the path, and for the thermal fusion between polymeric strings. In this way, a 3D object is made of 2D layers bonded together, and 2D layers are made of bonded thin strings.

The dispensing head is an important component of the 3D printer, having the role to melt and deliver the material for the 3D printed object (Fig. 1). The dispensing head ends with a conic-like nozzle that has a small hole in the tip (Fig. 2).

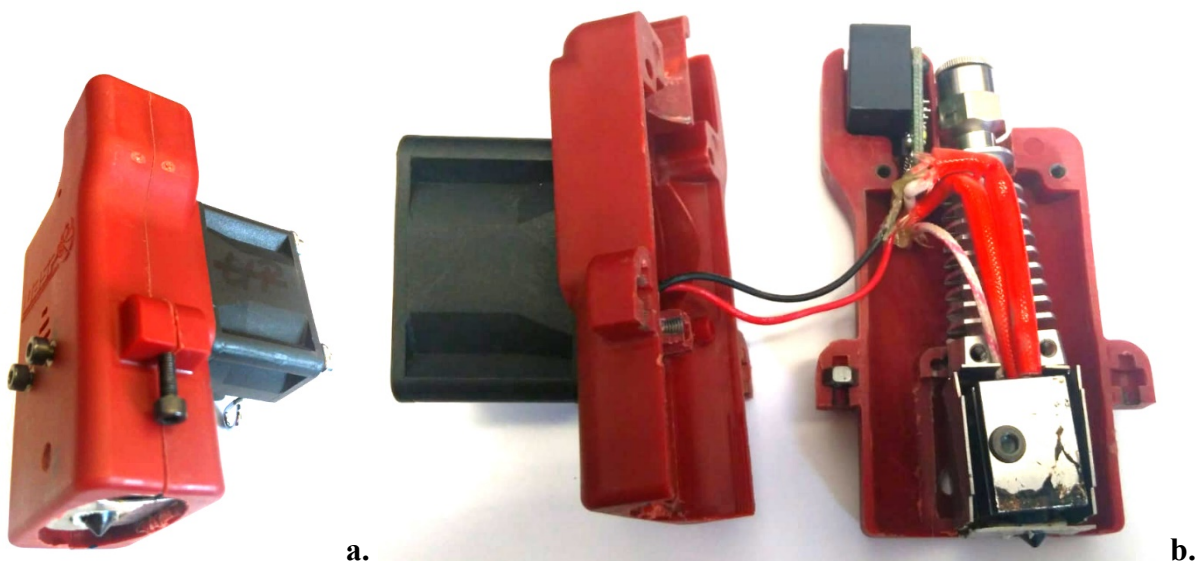


Fig. 1 Dispensing head of the polymeric strings (**a** – encapsulated, **b** - opened).



Fig. 2. Conic-like nozzle.

The hole's diameter ranges between 0.1 to 1.4 mm, with an increase step of 0.1 or 0.05 mm. The smaller the size of the hole, the higher the resolution of the 2D layer, but at the expense of increasing printing time. A smaller hole also requires a stronger pulling/pushing drive gear of the filament. Most of 3D printers work fine with a 0.4 mm nozzle. Different materials are used for making the nozzles, to provide either affordable price, or higher wear resistance, such as brass, steel, hardened steel, ruby, tungsten carbide, and others. The nozzle made of hard materials should be considered when printing with abrasive composite filaments. The nozzle must be heated to melt the filament. A cartridge heater (Fig. 3.a) is used to raise the temperature, usually to around 250-270 °C, depending on 3D printer and materials to be printed, and a thermistor measures the temperature of nozzle (Fig. 3.b).

An electronic circuit is used for amplifying the signal and transmitting the data (cartridge heater temperature, fan on/off, etc). The solid filament is pushed by a drive-gear through a tube, down to the hot nozzle. Depending on 3D printer design, the drive-gear can be separated by the hot-end or embedded together. The components are assembled on a frame, and cooled by a fan, which can also have the role to cool the melted filament. There are numerous designs, depending on producer. The challenge is to increase the working temperature to 500°C or even above, for printing with Polyether Ether Ketone (PEEK), Polyetherimide (PEI), or other high-performance thermoplastics.

The dispensing head is fixed on a support which is guided in a limited build space. Depending on mechanism, the header position can be controlled by combining 3 linear movements along X, Y, and Z axis (cartesian system, Fig. 4.a) or combining 3 linear vertical and independent movements (delta system, Fig. 4.b). Some other exotic mechanisms are proposed (e.g., polar, scara, robotic arm), but they remained part of more conceptual printers.



Fig. 3. Cartridge heater for filament melting (a) and thermistor for temperature measurement (b).

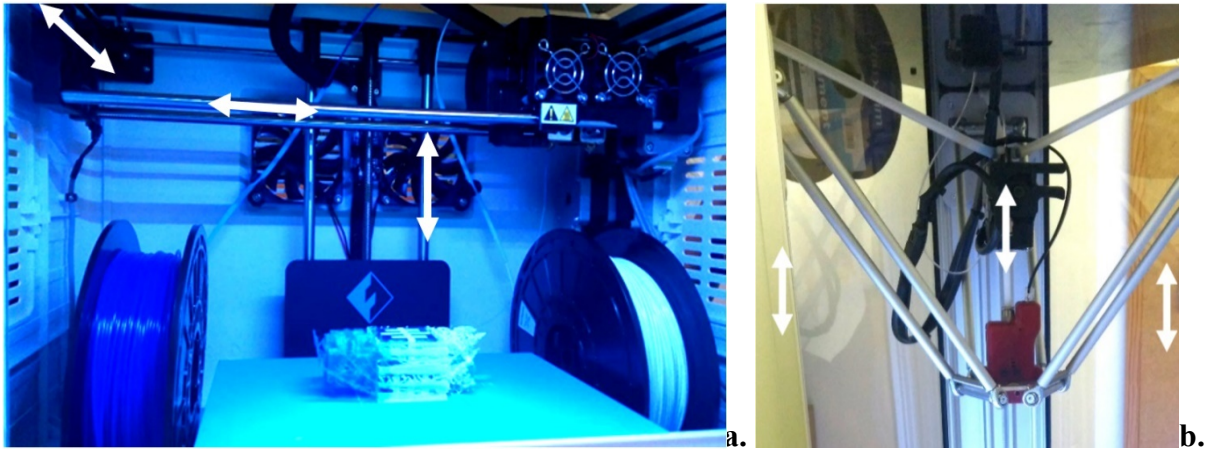


Fig. 4 Cartesian (a) and delta (b) systems of most used 3D printers.

The z resolution is given by the thickness of each layer, reaching down to 0.01 mm according with producers' specifications. In practice, the layer thickness is recommended to be about 80% of nozzle diameter. For example, for a nozzle of 0.4 mm diameter, the layer thickness should be 0.32 mm, and for a nozzle of 0.1 mm diameter, the layer thickness should be 0.08 mm. A certain resolution of a 3D printed object can be accepted if the size of the printed object is large enough. By FDM technology, very small objects cannot be printed at the highest printer resolution, e.g. a cube of $0.5 \times 0.5 \times 0.5 \text{ mm}^3$. Also, thin walls of an object will have a thickness equal to multiple of string thickness, otherwise empty space will be left (still the gaps can be filled using certain software options). On the other hand, a compromise between optimal resolution and time of printing is often made.

It is worthy to mention that recent 3D printers with two or more dispensing heads started to become popular. For dual dispensing heads one filament can be used for permanent deposition, and the second one for deposition of soluble supports. In other configurations, bicolor/multicolor objects can be printed. Regarding the physical parameters, for best results the operator should tune the working temperature of the extruder and the feed rate of the filament.

There are two main approaches for obtaining a 3D printed object. First route is to design a 3D virtual object using CAD (Computer Assisted Design) software, such as Autodesk Inventor, Fusion 360, SolidWorks, Catia, Rhino, FreeCad etc, either commercial or open-source (Fig. 5).

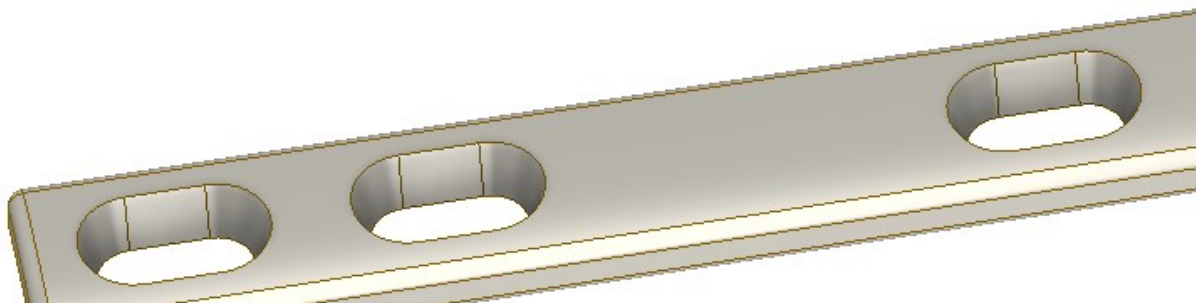


Fig. 5 Plate with slots for orthopedic use, designed with Autodesk Inventor 2020.

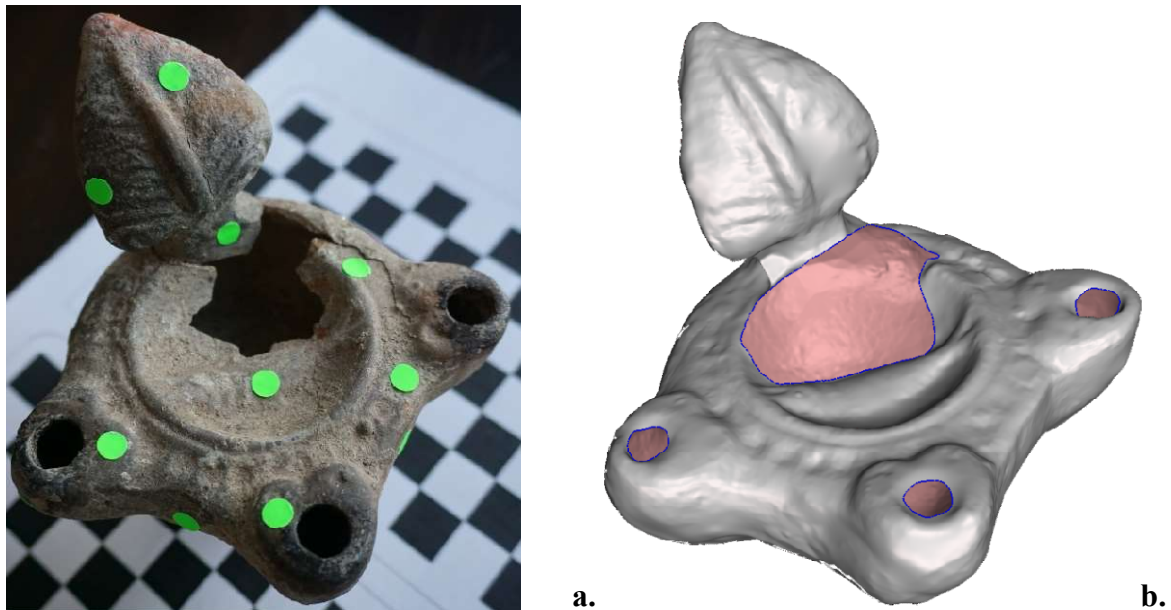


Fig. 6 Roman lamp from third century (a) and the corresponding 3D scanned image (STL file, where loss of details can be noticed, b).

Though each software has its own file type/extension, usually the virtual object can be exported as a *stl* file. STL stands for stereolithography, and the format carry the information about surfaces of a 3D object, each surface being composed of triangles. STL files can be saved/exported as ASCII or binary representations, the latter being more compact (much smaller size). STL files only represent the shape of the object, not the original colors or textures. The second route of obtaining STL files is by 3D scanning a real object and convert its shape into a digital one (Fig. 6).

Specialized software is used to analyze and enhance the STL file (Fig. 7), such as Meshmixer, Autodesk Netfabb, Meshlab, Materialise Magics, and many others. These applications are very useful to identify and repair some errors (e.g., holes in the surface, redundant surfaces, self-intersections) that can occur in the process of obtaining the STL file. Finally, once the clean/repared STL file is obtained, it is imported in another software for slicing and converting it into a *g-code* file. Some 3D printers can directly print STL files, but many of them work only with *g-code* files. Anyhow, *g-code* files are easy to read and modify, and this is useful for advanced modifications or research purpose. Advanced software integrate all functions, from importing STL to repairs and printing.

2.3 Production of filaments: technical approach, present status and future directions

Plastic industry is at a new crossroad in a world where white pollution became a real menace to our environment. It was reported an estimated quantity of 275 million metric tons of plastic waste in 2010, with 4.8 – 12.7 million metric tons found in the oceans (Jambeck et al., 2015). United Nations Environment Program reports an increase of interest for limiting single-use plastics and microplastics, and even ban the use of some products. While there is a decrease of using single-use plastics, the new 3D printing industry is counterbalancing the plastic industry by introducing on the market a new product: filaments of various materials for FFF/FDM 3D printing. Nevertheless, users of 3D printing technology

should be aware of toxicity that comes from decomposition of polymers, volatile organics and ultrafine particles (Stephens et al. 2013).

The technology for manufacturing plastic products is mature enough to easily shift from making bags, straws, etc to making 3D filaments. There is already a great boom in this industry, and very often a new type of filament (new colors, improved mechanical properties, new composites, new functions) is released on the market. The research in this direction is also spreading fast. From a research perspective, simple techniques for creating and testing new filaments are of main interest. Though sophisticated, fully automated extrusion machines already exist, for research purposes miniaturization is more desirable, as low quantities are required. Moreover, when nano-fillers are studied large extruders are not the best option. There are two main technical approaches for making filaments in a laboratory, considering the mixing of the starting raw materials.

The first one is a mechanical premixing of the pellets with the filler in a container, and then pour them in the extruder for a second mechanical mixing in the extruder. The second mechanical mixing will disperse the filler into the molten polymer, so the obtained filament will be a composite of the filler homogeneously dispersed in the polymer. If a better dispersion is required, the composite filament can be cut in small pellets and extruded again.

A second approach consists in dissolving the polymer in a solvent (e.g., PLA dissolves in chloroform), and add the filler in the resulted solution. Then slowly evaporate the acetone, while mixing the solution. Depending on the filler, dispersion can require more advanced techniques (ultrasonication, decreasing the viscosity of the solutions to avoid sedimentation of the filler). When dispersion of the filler is considered homogenous, the liquid composite will be spread in thin layers on a large support for a faster evaporation of the remnant acetone, and lower sedimentation. The dried composite will show porosity, but this will be eliminated in the extrusion step. It is important that all acetone to be evaporated before extrusion, otherwise the first filament will be porous. The dry thin layers are cut in small pellets for extrusion.

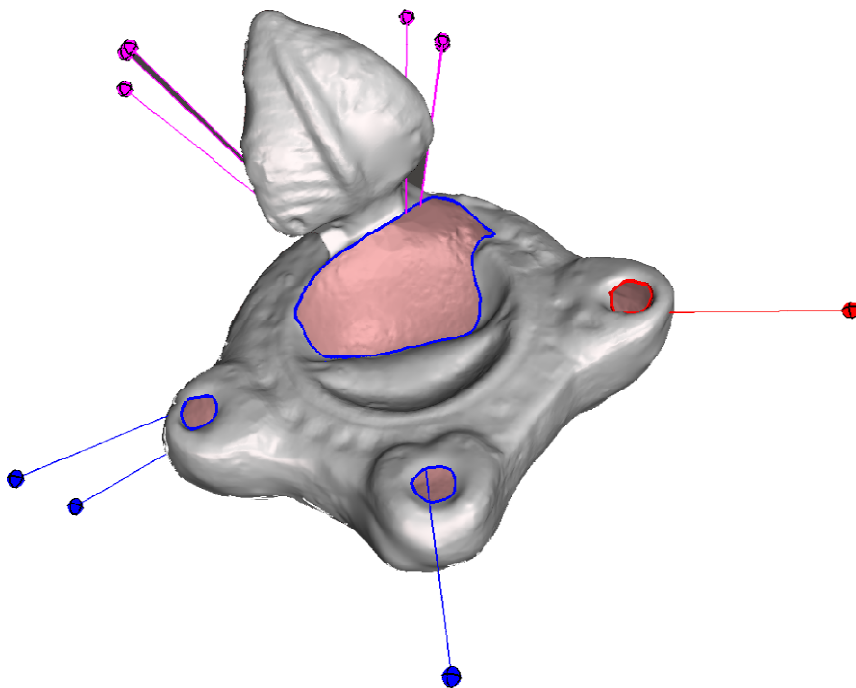


Fig. 7. Errors (holes) found with the Meshmixer software in the 3D scanned surface.

A second extrusion could be applied for elimination of the porosity or for a better dispersion of filler in the polymer.

For a good quality of 3D printing the obtained filament must have a constant diameter along its whole length. This is not an easy task even for an experienced researcher, especially when a new composite material is studied. Obtaining a filament with a constant diameter right from the extruder is almost impossible. Auxiliary devices are necessary, such as a cooling system (in air or water), a puller device to control the diameter of the wire (usually 1.75 mm), and a spinner to roll the wire. Also, various sensors are useful to control and tailor the parameters of the chained devices, such as the temperature of the extruder (with one to four heating areas), the temperature of the cooling system, the speed of the extruder motor, speed of the pulling device, speed of the roller. Some auxiliary devices for tensioning the filament, especially when working at high speed, could be also desirable. In the simplest configuration, at least 4 parameters should be adjusted for obtaining an almost constant diameter (temperature and speed of the extruder, temperature of the cooling system and the speed of the pulling system). The system can be automatically or manually operated, but in both cases many tests are necessary to optimize the process. Since the laboratory work is usually aiming the proof of concept, scaling to the industrial fabrication can totally change the working conditions.

Making the new filaments, though a time and effort consuming work, is just a small part of a research. Finding new or highly improved properties of the polymers/filaments, and finally of the 3D printed object, especially taking into the consideration the polymer-filler(s) long term reaction/adhesion and behavior, is the main work/research and the real challenge (De Franca da Silva Freitas, et al. 2017; Ulfah et al. 2015; Wang, 1998).

Currently there are many commercial thermoplastic filaments used for 3D printing, such as Acrylonitrile Butadiene Styrene (ABS), Polylactic Acid (PLA), Polyethylene Terephthalate Glycol-modified (PETG), Polycarbonate (PC), Acrylonitrile Styrene Acrylate (ASA), Thermoplastic Polyurethane (TPU), Nylon (Table 1), just to mention few.

From Table 1 we can observe that tuning the 3D-printer can sometimes be a trial and error method. The range of setting parameters (nozzle temperature, printing speed) are quite large and the experience of the operator and preliminary tests can hopefully tune the machine-material parameters for optimal results.

Composite filaments are also an attractive option on the market, either for esthetical purpose (e.g. PLA + wood fiber, stone/gypsum powder, bronze/steel/copper/brass powder), or because of their enhanced mechanical properties (e.g. carbon/glass fiber reinforced).

The challenge for 3D printing industry is to go beyond the hobby or the conventional approach of materials and to create new materials that can open new research directions and new applications by combining materials properties with complex shapes. Some current researches are about advanced composites materials for 3D printing, materials that exhibit shape memory effect (Yang et al. 2016), dielectric (Castles, et al. 2016), actuator (Correa et al., 2015; Le Duigou et al., 2016) or magnetic properties (Khatri et al, 2018).

There is a large spectrum of shape memory materials, such as cross-linked PE, trans-polyisoprene, styrene-based polymers, segmented polyurethane (Hu et al. 2012). Yang et al. reported DiAPLEX MM-4520 (a thermoplastic polyurethane elastomer type) pellets used for making the filament for 3D printing (Yang et al. 2016). The 3D printed objects exhibited shape memory effect at different temperatures. A dielectric composite based on ABS and

BaTiO₃ addition was proposed by Castles et al. (2016), that exhibited promising properties in different geometrical configurations.

Correa et al. (2015) and Le Duigou et al. (2016) presented an interesting approach: a wood fiber-polymer composite behaves as 4D material/printed object, where the 4th dimension is time, as the 3D printed object changes its shape or physical properties over time. The new material is hygroscopic and sensitive to humidity and temperature, being able to show different geometries influenced by external conditions. In Khatri et al (2018), an ABS-stainless steel composite filament was obtained, being useful for magnetic sensing applications.

2.4 Control parameters for high quality printing.

3D printing is a promising future technology, as part of the fourth industrial revolution. Conventional or unconventional 3D printers and dedicated materials are becoming more mature, meaning that we can acquire ready to print equipment. PLA and ABS are already easy printable materials, and finding optimal parameters is no longer a challenge, as the 3D printing software also offers optimized settings. Things are much different when it comes to print new materials, even pristine ones. Composite materials though are designed to enhance mechanical properties or deliver functional properties can require many tests for finding the adequate parameters. These parameters depend both on equipment performance, and materials properties.

The first condition to have a successful 3D printing is to provide a clean *stl* file, designed keeping in mind the possibilities and limits of a 3D printer. The next important condition is to provide good adherence of the material to the build platform (BP). First step, or the first layer is probably the most important. If the printed object does not firmly adhere to the build platform, it can be moved from the original position and the 3D printing fails. There are still many options to improve the adherence, such as (i) level the build platform to be in a horizontal position and the distance from the nozzle to be close enough, (ii) always adjust the temperature of the build platform according with the polymer type (e.g., 60 °C for PLA, 100 °C for ABS, 80 °C for PVA or Nylon, 100 °C for PMMA, but temperatures can strongly depend on each commercial filament, as different additions are used) and the melting temperature of the filament, (iii) increase the roughness of the building platform by grinding it with a fine sandpaper, spread a sticking film on the BP, use a special tape, clean the BP, (iv) tune the cooling fan speed, (v) tune the printing speed. Another solution is to increase the contact area with the BP by building rafts (an intermediate support between BP and 3D object), brims (outlines attached to the object) or skirts (outlines around the rafts that clean the nozzle and provide a constant flow). Sometimes, using BP of a specific material can help for a better adhesion, for example borosilicate glass, with a very low thermal expansion, works fine with ABS. Large shrinkage of 3D printed objects leads to warping effect (Fig. 8). Hence an improved adhesion of the first layers is critical. For avoiding large shrinkage of 3D objects, 3D printers are usually encased in a chamber for a better temperature distribution.

Once the adherence is solved, next essential parameter to set is the melting temperature of the filament. The melting temperature can depend not only on the material (Table 1), but also on the filament thickness.

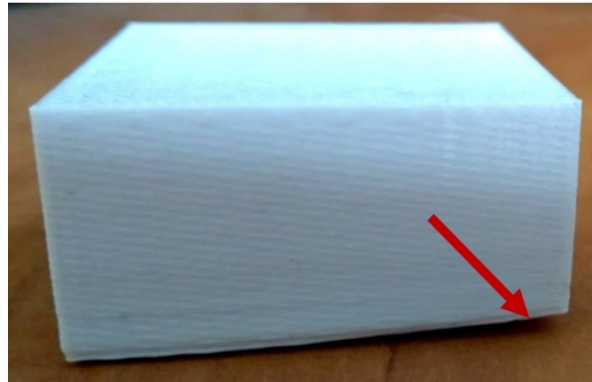


Fig. 8. Large warping effect on a PLA 3D printed cuboid due to shrinking and poor adhesion.

If the filament is thicker, the temperature should be slightly higher. The operator should test within the temperature range recommended by the producer (usually start with the average) and depending on the print quality or equipment decide the optimal temperature. An optimal temperature will provide a smooth flow of the filament. If the temperature is too high the filament tends to spread, while if it is too low the filament will tend to cool down too fast to properly stick to previous strings/layers. In PMMA case, if the temperature is too low, the strings will start curling.

Though each software will correlate the nozzle diameter with the filament thickness and printing speed, still some parameters can be manually modified for a fine tuning of printing quality. One important parameter is the extrusion multiplier, that can tune the flow rate of the printed string. If some gaps are observed between the melted strings (Fig. 9), then we have an under-extrusion, and the flow rate should be increased. If the flow rate is too high, then we have an over-extrusion, which usually will affect the quality of the walls.

The gaps between walls can occur due the assigned thickness of the walls in the CAD software. For a good quality of the 3D object, the designer should correlate the dimensions of the digital object with the performance and resolution of the 3D printer.

Table 1. Commercial polymers and recommended 3D properties (based on commercial Polymaker data, average values).

Polymer	Nozzle temperature, [°C]	Printing speed, [mm/s]	Build platform temperature, [°C]	Cooling fan	Filament drying conditions	Young Modulus, [MPa]	Tensile strength, [MPa]	Bending strength, [MPa]	Charpy impact strength, [kJ/m ²]
ABS	245-265	30-50	90-100	OFF	8h at 80 °C	2174	33	59	13
PLA	190-230	40-60	25-60	ON	8h at 80 °C	1879	28	48	12
PETG	230-240	30-50	70-80	ON	8h at 70 °C	1472	32	54	5
PC	250-270	30-50	90-105	OFF	8h at 80 °C	2048	60	94	25
ASA	240-260	30-50	75-95	OFF	8h at 80 °C	2379	44	73	10
TPU	210-230	20-40	25-60	ON	12h at 70 °C	-	29	-	-
Nylon	250-270	30-50	25-70	OFF	12h at 80 °C	2223	66	97	10

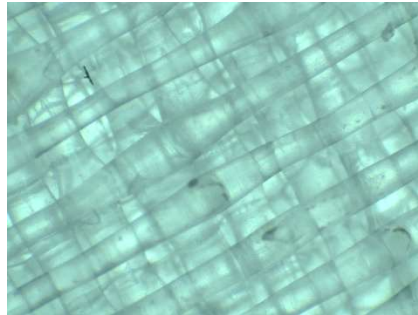


Fig. 9. Under-extrusion of deposited melted filament.

For avoiding the gaps between outline/perimeter shells (Fig. 10.a, b), either we can adjust the wall thickness using the CAD software, or just check some additional 3D printing options in the software (Fig. 10.c, d). A preview of the printing simulation is useful, and it is important to attentively read and analyze the simulated result. This can save much effort and time. There are different calibration tools or *stl* files designed by passionate 3D printer operators, as well as a large 3D printing community, to help the operator to print and figure out the best parameters for obtaining high quality objects, with smooth surface, good fusion, lack of artifacts, excellent mechanical or functional properties. It is important to understand that 3D printing technology is not a "one-click" technology, and constant effort, tests, failures, analyzes are required to obtain the desired object or material.

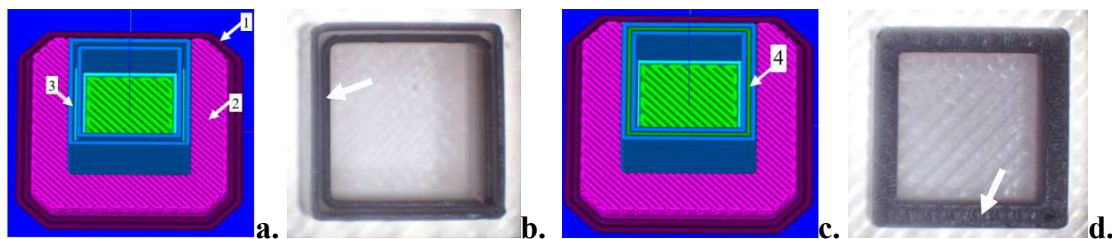


Fig. 10. **a.** Brim (1) around the raft (2) and gaps (3) between the outline shells. **b.** The 3D printed object with gaps between outline walls. **c.** Filled gaps (4) using advanced option (allow single extrusion wall) in Simplify3D software. **d.** Filled gaps between outline walls.

3 Green Polymers

Green polymers are numerous, and they are obtained with various ways. Av erou (2004) have proposed to class the biodegradable polymers in function of their synthesis and their origin in four groups (Fig. 11).

- Group 1: Polymers derived from biomass. On the one hand one, it is polysaccharides such as starch, cellulose, lignin, ... and on the other hand, it is animal or vegetable proteins,
- Group 2: Polymers produced by microorganisms and obtained by extraction: polyhydroxyalkanoates (PHA)

- Group 3: Polymers derived from biotechnology. They are produced by conventional synthesis from monomers derived from renewable resources, such as polylactic acid (PLA)
- Group 4: Polymers whose monomers come from fossil resources and which are obtained by conventional synthesis. They are polyesters such as poly (ϵ -caprolactone) (PCL), polyesteramides and aliphatic copolyesters (PBSA) or aromatic.

In this chapter only PCL will be discussed. In the production of these polymers, green principles are: a clean production process, no use of additional substances such as organic acids, high content of raw material, energy efficiency of the manufacturing, use of renewable resource and/or energy, lack of environment hazards, controlled lifecycles, low carbon footprint and high safety standards.

3.1 Polymers from petrochemical synthesis (group 4): Polycaprolactone (PCL)

Poly(ϵ -caprolactone), often simply termed polycaprolactone and abbreviated as PCL, is a biodegradable aliphatic polyester that is semi-crystalline. It is composed of hexanoate repeated units (Fig. 12). There are two methods to synthesize PCL: the polycondensation of 6-hydroxycaproic (6-hydroxyhexanoic) acid and the ring-opening polymerisation (ROP) of ϵ -caprolactone (ϵ -CL, a cyclic monomer). Both 6-hydroxyhexanoic acid and ϵ -CL can be obtained as intermediate products during the oxidation of cyclohexanol into adipic acid by a number of microorganisms, such as *Acinetobacter* sp. strain SE19 (Thomas et al., 2002).

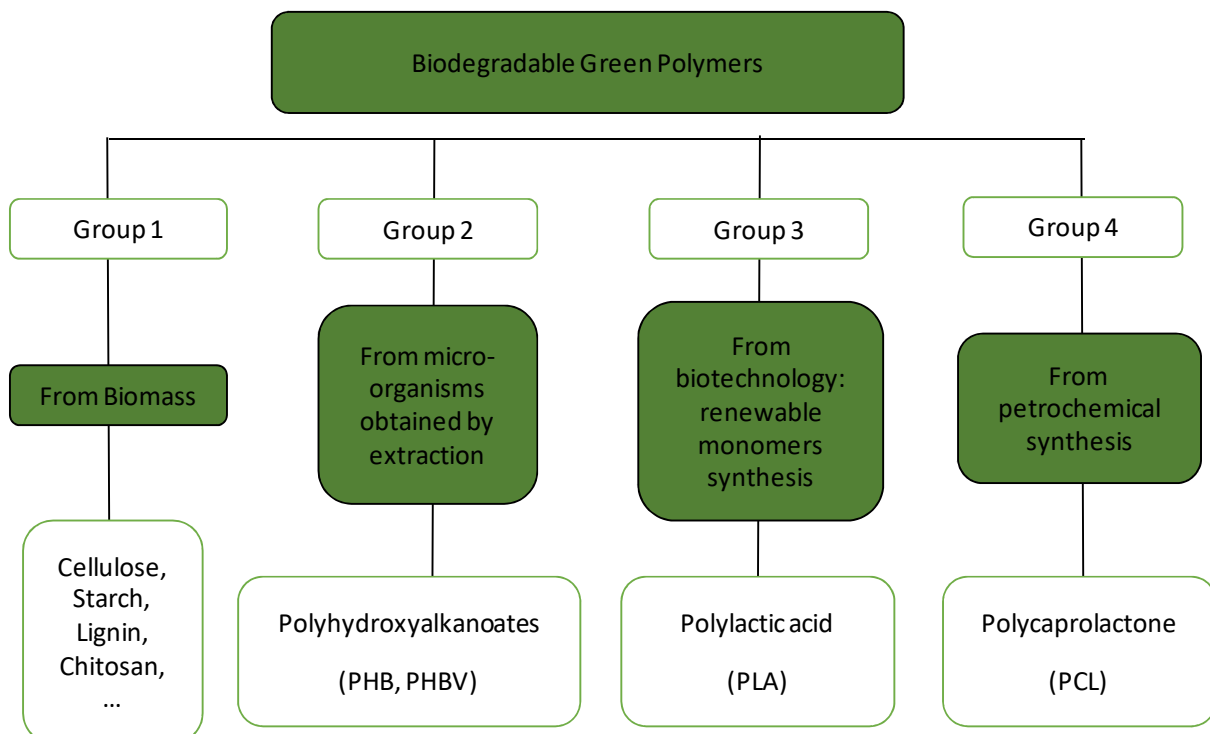


Fig 11 The 4 groups of biodegradable green polymers adapted to Avérous, 2004

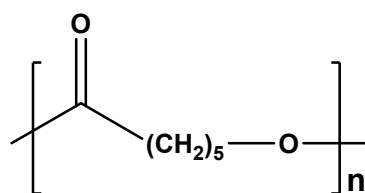


Fig 12. Polycaprolactone polymer chain.

But at an industrial scale, ϵ -CL is produced from the oxidation of cyclohexanone by peracetic acid (Labet and Thielemans, 2009). Of the two synthesis routes, the main one is the ROP of ϵ -CL since it allows higher molecular weight PCL chains and lower polydispersity. Four main mechanisms for the ROP of lactones exist, and they depend on the catalyst: anionic, cationic, monomer-activated and coordination-insertion ROP, a large number of catalysts and catalytic systems, spanning virtually the whole periodic table having been investigated. The catalyst is mainly chosen for the particular application and the targeted reaction condition, the different ROP mechanisms affecting the resulting molecular weight, molecular weight distribution, end group composition (Okada, 2002). More informations on the reaction mechanisms can be found in the review from Labet and Thielemans (2009). The chain termination step usually requires the addition of an acid or of low molecular weight alcohols to control the molecular weight of the obtained polymer chains.

PCL is semi-crystalline with a degree of crystallinity reaching up to 69 % depending on the thermal treatment applied – slow crystallization or melt quenched cooling, even higher values having been obtained by rearrangement of the chains in solution after slow solvent evaporation (Más Estellés et al., 2008). PCL has a density of around 1.2 g.cm^{-3} . Its number average molecular weight (M_n) may generally vary from 3000 to 80,000 g/mol, with crystallinity decreasing with increasing molecular weight. Depending on its crystallinity and M_n , PCL melting point ranges between 59 and 64°C, making it a “safe” thermoplastic to print. It has a low glass transition temperature (T_g) of -60°C meaning PCL is always in a rubbery state at room temperature, an unusual property among aliphatic polyesters, making the product extremely flexible and tough [28]. PCL starts decomposing at 250 – 350°C, with full decomposition being obtained above 500°C according to thermogravimetric analyses (PCL $M_n = 50\text{k}$) (Lepoittevin et al., 2002). PCL is hydrophobic owing to its large water contact angle and it is insoluble in water, alcohols, petroleum ether, diethyl ether. On the other hand, it is soluble in chloroform, dichloromethane, carbon tetrachloride, benzene, toluene, cyclohexanone, 2-nitropropane, THF; slightly soluble in acetone, 2-butanone, ethyl acetate, dimethylformamide, aceto- nitrile.... PCL demonstrates quite a unique ability to form compatible blends with a wide range of other polymers, e.g. to improve stress crack resistance, dye-ability and adhesion (Engelberg and Kohn, 1991). It has been used in association with cellulose propionate, cellulose acetate butyrate, PLA and PLGA (Chandra and Rustgi, 1998). ϵ -caprolactone can also be copolymerized with a variety of monomers including ethylene oxide, polyvinylchloride, chloroprene, polyethylene glycol, polystyrene, urethanes, tetrahydrofuran, diglycolide, dilactide, valerlactone, substituted caprolactones, 4-vinyl anisole, styrene, methyl methacrylate and vinyl acetate, yielding PCL copolymers (Okada, 2002; Woodruff and Hutmacher, 2010).

The rheological properties of PCL are depending whether temperature is above or below melting point (60°C). Chen et al. (2005) performed the dynamic mechanical thermal analysis

(DMTA) of PCL ($M_n = 80k$) in tensile mode, within a range of temperature investigated from -100 to $+50^\circ\text{C}$. At an oscillation frequency of 1 Hz, they observed the storage modulus E' decreasing from 3 GPa at -100°C to 0.3 GPa at $+50^\circ\text{C}$, while the loss modulus E'' decreased from 0.15 GPa at -100°C down to 0.05 GPa at $+50^\circ\text{C}$. The peak transition temperature in the $\tan \delta$ curve (maximum value of $\tan \delta$ associated to the glass transition resulting in an increase in the viscous behavior) is found to be higher than the peak temperature in the E'' curve, which is characteristic of semi-crystalline polymers.

PCL exhibits a sharp decrease in the modulus values above 55°C , due to the onset of melting of the polymer (Mittal et al., 2015). The effect of the molecular weight on the rheological properties of PCL melts were examined in a reference study by Grosvenor *et al* (1996) who investigated M_w in the range 17k to 36k with polydispersity between 1.7 and 1.9. PCL melts with low M_w ($< 25k$) showed only a slight deviation from a Newtonian behavior, with viscosity remaining nearly constant with increasing shear rate. In contrast, for $M_w > 30k$ a non-linear shear stress/shear rate relationship typical of a pseudoplastic flow behavior was observed, with the viscosity decreasing with increasing shear rate. Apparent melt viscosity at 70°C ranged from 30 Pa.s up to 300 Pa.s, and at 100°C ranged from 20 Pa.s up to 125 Pa.s, the lowest values being obtained for low M_w , poorly crystalline PCL, an intuitive result since less thermal energy is required to disentangle short polymer chains compared to larger ones; since the degree of entanglement is generally a function of polymer chain length, the shorter the length (low M_w) the lower the viscosity (Graessley, 1967). Concerning the dynamic rheological properties of high molecular weight PCL melts, at low frequencies the melt behaves like a Newtonian fluid while at relatively high frequencies it exhibits a pseudo-plastic behavior. Hence for oscillation angular frequency increased from 1 to 100 rad/s, Chen and Sun (2005) observed the storage modulus G' to increase from 4 kPa to 400 kPa and the loss modulus G'' to increase from 15 kPa to 300 kPa, while the viscosity decreased from 15 kPa.s to 5 kPa.s (PCL $M_n = 80 k$ at 110°C). Similarly, for PCL $M_n=50k$ at 80°C , Lepoittevin *et al* (2002) found G' to increase from 100 Pa to 80 kPa and G'' to increase from 2 kPa to 100 kPa with increasing angular frequency (from 1 to 60 rad/s).

PCL is compostable under home composting conditions, a reason why it has been used as a biodegradable packaging material (Engelberg and Kohn, 1991). Depending on its molecular weight, degree of crystallinity and conditions, its degradation can take several months to years, being significantly slower than that of PGA or PLA (Gross and Kalra, 2002). Many microbes in nature are able to completely biodegrade PCL. The amorphous phase is degraded first, resulting in an increase in the degree of crystallinity while the molecular weight remains constant (Lam et al., 2007). Then, cleavage of ester bonds results in mass loss (Peña et al., 2006). At low temperature, the polymer chain degrades by random scission while at higher temperatures end chain scission occurs (Joshi and Madras, 2008). High molecular weight PCL takes much longer to degrade: the larger the chain length, the greater the number of ester bonds to be cleaved before obtaining water-soluble monomers/oligomers allowing surface erosion to proceed. Like other polyesters, PCL degradation is auto-catalysed by the carboxylic acids liberated during hydrolysis, but several enzymes can also act as catalyst and speed up the decomposition in the environment (Labet and Thielemans, 2009). PCL is also bioresorbable, meaning that it is entirely eliminated from the body through natural pathways, including its degradation by-products, with no residual side-effects. After the non-enzymatic hydrolytic cleavage of ester groups, once the polymer has become more highly crystalline and of low molecular weight ($M_n < 3000$), PCL *in vivo*

undergoes intracellular degradation as evidenced by the uptake of PCL fragments in phagosomes of macrophages, giant cells and within fibroblasts (Woodward and al., 1985). Indeed, the hydrolysis of PCL yields 6-hydroxyl caproic acid and acetyl coenzyme A which enter the citric acid cycle and through this metabolic pathway are eliminated from the body (Albertsson and Karlsson, 1996). A 3-years follow-up study showed that PCL with an initial Mw = 66 kg/mol remained intact in shape during the first 2 years of implantation, then broke into low Mw (8 kg/mol) pieces after 30 months. The Mw continued to linearly decrease with time. Using radioactive labelling, it was shown that more than 90% of the labelled-PCL was excreted from feces and urine, while radioactivity in the organs remained close to background level, evidencing that PCL did not accumulate in body tissue and could be completely excreted (Woodruff and Hutmacher, 2010; Sun et al., 2006).

The properties of PCL make it particularly suitable for additive manufacturing and especially for FDM which the most commonly used and affordable printing technique is. PCL has high adhesion between layers, improving the impact resistance, strength, durability of the fabricated object. Due to the low melting point of PCL, the objects can be re-shaped after printing to fit specific application by simply softening it in warm (60°C) water. It can be processed at much lower and safer temperatures (70°C to 140°C) compared to the commonly used PLA or ABS polymer and does not require a heated bed. Details on the set-up parameters depending on the printing technique are given below in Table 2.

PCL filaments are also commercially available under a 1.75 mm diameter; their molecular weight is rarely specified, although it should presumably be comprised between 50k to 80k. Some suppliers are Polyfluor Plastics, Filaments.ca and commercial brand names include FACILAN™ PCL100 and FACILAN™ ORTHO by ElogioAM, "Flexible Filament" by Makerbot, eMorph and eMate by eSun. For most of FDM printers equipped with a 400 µm nozzle, PCL prints best at approximately 140°C with a bed temperature between RTP to 38°C and a speed of 30 mm/s. Since PCL flows extremely easily through the nozzle at 140°C it is necessary to cool it down quickly to fix the print, therefore best results are obtained with fans at 100% (from Elogio AM tech sheet recommendation https://cdn.shopify.com/s/files/1/0108/1881/4009/files/TDS_Facilan_PCL100_ElogioAM_V1.4.pdf?4463025051778730948).

FDM generally involves the use of a filament, although a variant of the technique (sometimes denoted as Precision Extrusion Deposition, PED) allows the printing from raw PCL powders. Fabrication of the filament implies the hot extrusion of PCL through a 1.75 mm nozzle using a screw extruder at a temperature above 70°C. This can lead to small changes in the mechanical properties of the extruded PCL filament. For information, the properties of a commercially available filament are provided on the technical data sheet from the supplier (https://cdn.shopify.com/s/files/1/0108/1881/4009/files/TDS_Facilan_PCL100_ElogioAM_V1.4.pdf?4463025051778730948). Overall, the mechanical properties of the source PCL before and after extrusion remain in the range shown in Table 3, although it is advisable to monitor the possible change in the PCL molecular weight resulting from the additive manufacturing process, which can be deduced e.g. from Gel Permeation Chromatography.

Table 2 Print parameters investigated an suitable for PCL

⁽¹⁾: Hendrikx et al., 2016; ⁽²⁾: Kosik-Kozioł et al., 2019; ⁽³⁾: Gómez-Lizárraga et al., 2017; ⁽⁴⁾: Woodruff, et al. 2010 ; ⁽⁵⁾: Neufurth et al., 2017; ⁽⁶⁾: Szojka et al., 2017

3D printing temperature	75°C ⁽¹⁾ -115°C ⁽²⁾
3D printing speed	0.5 mm.s ⁻¹ – 5 mm.s ⁻¹ ⁽³⁾
Heated bed temperature	Ambient ⁽⁴⁾
Extrusion pressure	1-8 bars ⁽⁵⁾
Pre-flow delay	0.3 s ⁽⁵⁾
Post-flow delay	0.5 s ⁽⁵⁾
Wait time between layer	5 s ⁽⁵⁾
Interlayer overlap	20 – 33% ⁽⁵⁾
Needle gauge (inner diameter)	0.178 μm – 800 μm ⁽³⁾
Needle length	3 mm ⁽⁶⁾

Table 3 Summary of PCL properties (Bossard et al., 2018; Chun et al., 2015; Labet and Thielemans, 2009;, Kosik-Kozioł et al., 2019; Salin and Seferis, 1993; Wang et al., 2015)

Density	1.07 – 1.2
Crystallinity	up to 70%
Lattice parameter	a = 7.496 Å, b=4.974 Å, c (fibre axis) =17.297 Å
Number average molecular weight	Mn = 530 – 630 000 g/mol
Tensile strength	σ = 4 – 780 MPa
Tensile modulus	E = 210 – 440 MPa
Elongation at break	ε = 20 – 1000 %
Water contact angle	74 – 79°
Glass transition Tg	(– 65 °C) – (– 60 °C)
Melting point Tm	56 – 65 °C
Decomposition temperature	250 – 350 °C
Crystallization temperature Tc	20 – 37°C
Theoretical heat of fusion for 100% crystalline PCL	136 J/g
Degradation time in the environment	months to years
Resorption time in the body	years
Solvents	highly soluble in chloroform, dichloromethane, carbon tetrachloride, benzene, toluene, cyclohexanone, 2-nitropropane, THF; slightly soluble in acetone, 2-butanone, ethyl acetate, dimethylformamide, aceto- nitrile
Non-solvent	alcohols, petroleum ether, diethyl ether, water
Commercial brand names	Capronor, CAPA, Polymorph, Plastimake, NiftyFix, Protoplastic, InstaMorph, Shapelock, ReMoldables, Plastdude, TechTack...

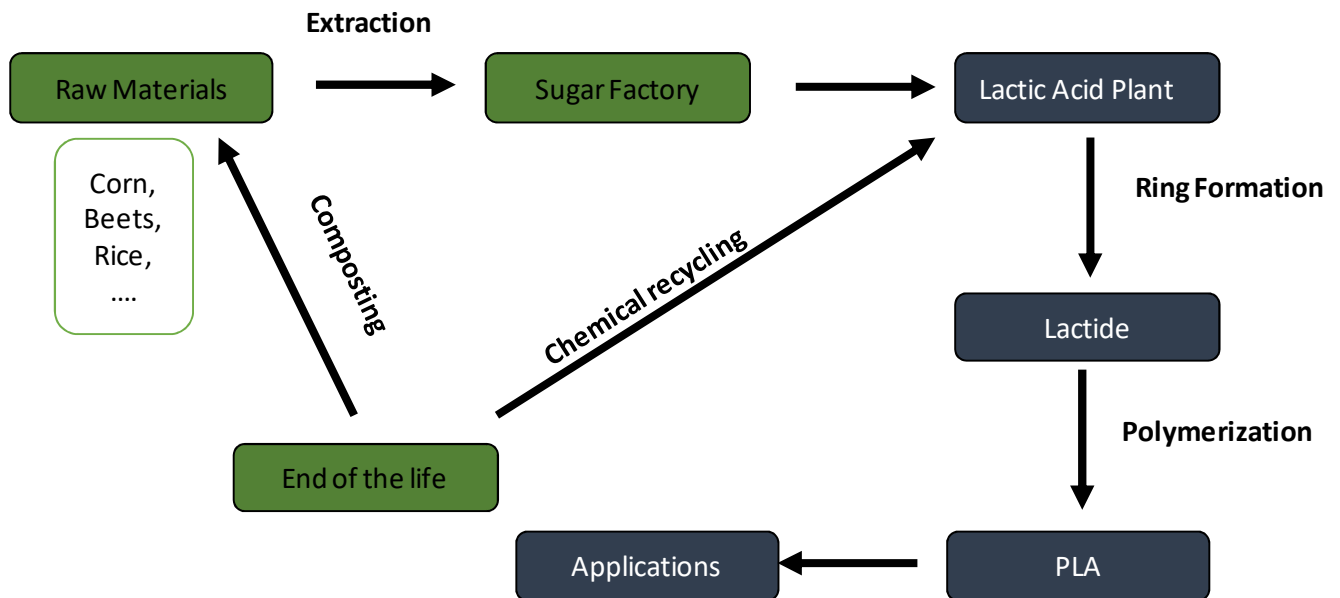


Fig 13 PLA life cycle schematic diagram

3.2 Polymers from biotechnology (group 3)

3.2.1 Polylactic acid (PLA)

Poly (lactic acid) or polylactide (PLA) is probably the most used of green polymers for filaments. This polymer is vegetable origin (corn starch, beets...), biodegradable and nontoxic. It is used in various applications: biomedical, packaging, textile fibers, technical items... PLA is hydrophobic and water resistance. All PLA are insoluble in water, some alcohols and alkanes. In general, PLA is soluble in dioxane, acetonitrile, chloroform, methylene chloride, 1,1,2-trichloroethane and dichloroacetic acid (Madhavan Nampoothiri et al. 2010).

Polylactic acid is generally synthesized from α -hydroxyacids (Garlotta, 2001). Lactic acid or 2-hydroxypropanoic acid is obtained from sugar or starch fermentation (Fig. 13). The basic building block for PLA is lactic acid which can be manufactured either by carbohydrate fermentation or chemical synthesis. The most commonly used industrial method is the ring opening polymerization (Fig. 14). In a first step, a prepolymer is produced by polycondensation of lactic acid (high temperature and low vacuum conditions). This prepolymer has a low molecular weight ($M_w < 1000 - 5000$ Da). The second step consists in the depolymerisation of the prepolymer to obtain lactide. Lactide is formed by different isomers: L-Lactide, D-lactide and meso-lactide. Ring opening polymerization of lactide leads to high molecular weight PLA ($M_w > 100\,000$ Da). PLA forms a chiral molecule with two stereoisomers: L-lactic acid and D-lactic acid (Fig. 15). PLA properties depend principally of the ratio between L- and D- lactic acids. PLA which contain a large part of L-lactic acid (>93%) are semi-crystalline while PLA which contain between 50% and 93% of L-lactic acid are totally amorphous (Auras et al., 2004). Semicrystalline PLA and amorphous PLA have glass transition temperature (T_g) and melting temperature (T_m) slightly different. Glass transition temperature and melting temperature are function of the initial monomeric composition

and the molecular weight. They also depend of the molecular flexibility and geometry and the intermolecular forces. Its leads to higher values for semicrystalline PLA. In his review, Garlotta (2001) said the melting temperatures of pure D lactide and pure Lactide were the same (207°C) but typical melting temperatures of PLA were in the 170-180°C range. He attributed this to small and imperfect crystallites, slight racemization and impurities.

Poly -L-Lactic acid (PLLA) has a crystallinity of around 37%, a melting temperature between 170 – 183°C (Gupta and Kumar, 2007) and a glass transition temperature between 50-80°C while Poly (D,L-lactic acid) (PDLA) has a glass transition temperature between 55 – 65°C (Madhavan Nampoothriri al al., 2010).

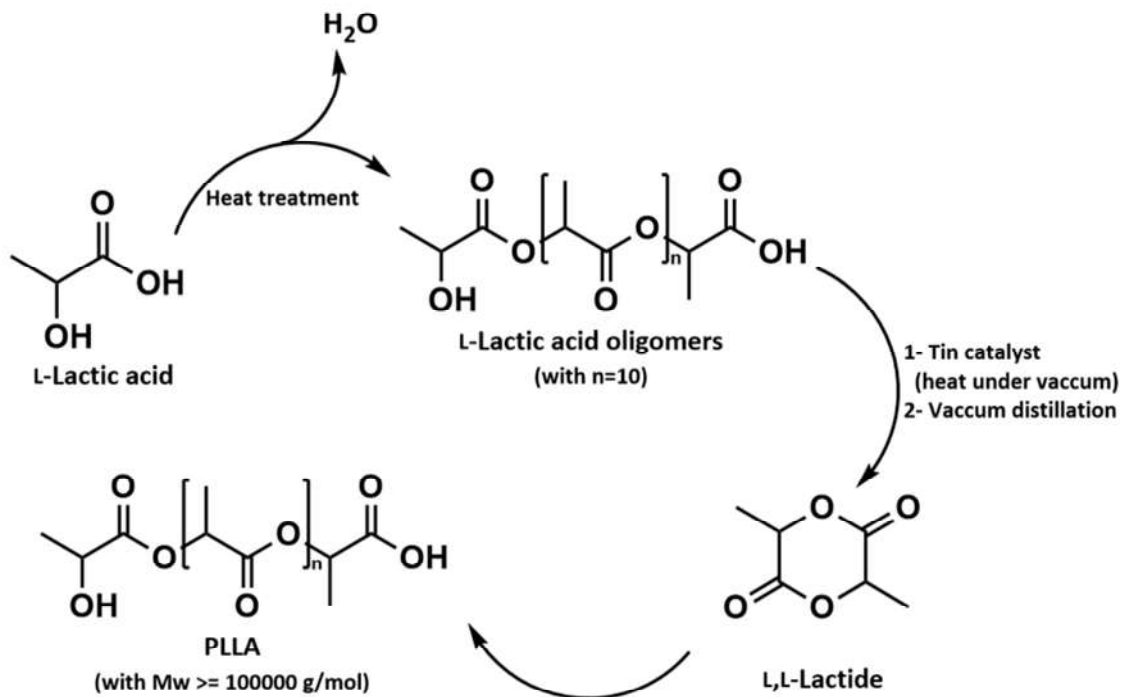


Fig 14. PLLA manufacturing process.

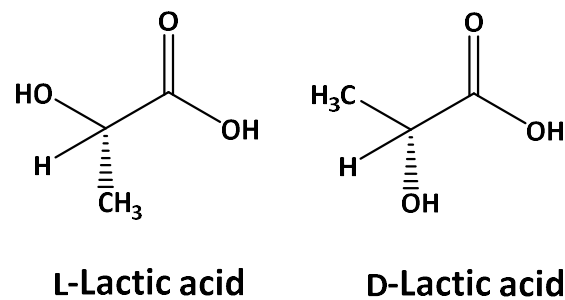


Fig 15. Representation of the two stereoisomers of PLA: L-lactic acid and D-lactic acid.

Fang and Hanna, (1999) determined glass transition and melting temperatures of 58°C and 148°C respectively for amorphous PLA (82% of L-lactide and 18% of D-lactide) while they are of 62°C and 151°C, respectively for PLA (95% of L-lactide and 5% of D-lactide). J. Dorgan et al. worked with commercial grade of lactic acid (Cargill-Dow Polymers) (96% of L-lactide and 4% of D-lactide) and they obtained a Tg of 58.4 °C and a Tm of 151.7°C (Dorgan et al., 2000). For Jamshidi et al. (1988), glass transition temperature is not affected by the molecular weights of PLA. They found a Tg of 55°C for PLA with a molecular weight of 22,000 g/mole and the predicted value of PLA with infinite molecular weight is only to 4-5°C upper. On the contrary, Dorgan et al. have shown the PLA glass transition temperature depended of L-isomer content and molecular weight (Dorgan et al., 2005). Among the commercial filaments, Nature works PLA has a glass transition temperature of 55-56 °C et Biomer L9000 PLA has a VCAT softening point of 56°C (Madhavan Nampoothiri, 2010). The disadvantage of PLA is its low heat distortion temperature with behavior above 60°C. Melt flow rate (MFR) depends of PLA. For example, PLA Biomer L9000 (Biomer, Germany) has a MFR in range 3-6 g/10 min. MFR for Nature Works PLA ® (NatureWorks LLC is between 2.3 and 4.3 according to Madhavan Nampoothiri (2010). while it is estimated to 6g/10 min (2,6 kg, 210°C) according to Peinado et al. (2015).

Rheological properties are strongly depended of PLA structure and conditions of implementation (temperature and shear rates). PLA is a thermoplastic polymer, so it exhibits two behaviors in function of the shear rates. For low shear rate ($<10 \text{ s}^{-1}$), high molecular weight PLA presents a Newtonian behavior whereas at high shear rates ($>10 \text{ s}^{-1}$), it presents a non Newtonian behavior (Hamad et al., 2015). As the shear rates increase, the viscosity of high molecular weight PLA melt decreases significantly. An explication is a strong shearing action can break the molecular chains of the polymer (Fang and Hanna, 1999). On the other hand, low molecular weight has a quasi Newtonian behavior at shear rates typical of film extrusion (Copper-White and Mackay, 1999). Temperature influences too the viscosity. This one decreases when the temperature increases. The effects of the composition (L and D lactides) influence also the results. It has been shown that the shear viscosity of PLA increases when the % of L lactide increased i.e. when the crystallinity increased (Dorgan et al., 2000; Fang and Hanna, 1999).

When exposed to elevated temperature, PLA is known to undergo thermal degradation. The decrease of the molecular weight depends in the process temperature, the residence time in the extruder and the shear stress. The reactions are numerous: hydrolysis by trace amounts of water, depolymerization according to back-sitting mechanism, oxidative, random main-chain scission, intermolecular transesterification to monomer and oligomeric esters and intramolecular transesterification resulting in formation of monomer and oligomer lactides of low molecular weight (Kopinke et al., 1996; Lim et al., 2008). Also, to reduce PLA thermal degradation, it is recommended to correctly dry the PLA before its implementation to avoid the hydrolysis reaction during the melt processing. Natureworks LLC, one of the main suppliers for PLA polymers, recommended that PLA is dried to below 0.025% w/w. moisture content before extrusion (Lim et al., 2008). Drying conditions are dependent on temperature, air flow rate and dew points (Jamshidian et al., 2010). For example, amorphous PLA in the form of pellets must be dried below the glass transition temperature. Above, pellets can stick together. For semicrystalline PLA, drying conditions are recommended with temperatures range between 80 to 100°C and times range between 4 to 2h. After drying, PLA pellets must be conserved in sealed packages to prevent moisture from atmosphere.

Comparatively to traditional polymers, PLA has good properties and close to polystyrene. PLA tensile strength and Young's modulus are high. For example, Young's modulus of PLA is 3.8 GPa while Young's modulus is 3.39 GPa for polystyrene and 1.4 GPa for polypropylene. PLA has a good flexural strength but a very low elongation at break: 4 % for PLA versus 2% for polystyrene and 400 % for polypropylene (Dorgan et al., 2000). PLA is a relatively brittle plastic that limits its utilization. In fact, mechanical properties depend of the molecular weight and the treatment after implementation, annealing for example. Perego et al. (1996) results are summarized in the Table 4. Mechanical properties of higher molecular weight PLA were better than those of lower molecular weight PLA. After an annealing at 105°C during 90 min under nitrogen, the strength increased probably because of the increase of the crystallinity. Izod impact is defined as the kinetics energy needed to initiate failure and continue the fracture until the specimen is broken. Two tests exist: notched and unnotched Izod Impact tests according to the preparation of the specimen. Nature of PLA (L or L/D PLA) and thermal treatment (annealing or not) influence the material resistance to impact as it is summarized in the Table 5.

Table 4 Mechanical properties of Poly(L-lactide), annealed Poly(L-lactide) and Poly(D-L Lactide) specimens (Perego et al., 1996)

Sample	Low Mw PLLA	High Mw PLLA	Low Mw annealing PLLA	High Mw annealing PLLA	Low Mw PDLLA	High Mw PDLLA
Mw	23 000	67000	20 000	71 000	47 500	114 000
Yield strength (MPa)	-	70	-	70	49	53
Tensile strength (MPa)	59	59	47	66	40	44
Yield elongation (%)	-	2.3	-	2.0	1.7	1.5
Elongation at break (%)	1.5	7.0	1.3	4.0	7.5	5.4
Young modulus	3550	3750	4100	4150	3650	3900
Flexural strength (MPa)	64	106	51	119	84	88
Maximum strain (%)	2.2	4.7	1.6	4.6	4.8	4.2
Modulus of elasticity (MPa)	3650	3650	4200	4150	3500	3600

Table 5 Influence of nature and thermal treatment on unnotched and notched Izod Impact (Garlotta et al., 2001).

	L-PLA	Annealed l-PLA	D,L-PLA
Unnotched Izod Impact (J/m)	195	350	150
Notched Izod Impact (J/m)	26	66	18

Valorization of PLA wastes were studied by Piemonte (2011). Four scenarios were studied: incineration, composting, anaerobic digestion and mechanical recycling. The last scenario was estimated the best alternative from an environmental point of view. Much of commercial filaments come from recycling. However, literature reports an important decrease of the PLA molecular weight, an increase of crystallization (Brüster et al., 2016; Pillin et al. 2008) , a decrease of the tensile stress after few mechanical recycling processes (extrusion process and injection process) (Zenkiewicz et al., 2009). But in these studies, degradation PLA during its service life was not considered. Beltran et al. have studied the effect of degradation during use from an accelerated ageing and introduced a demanding washing process before a second melt processing step.

They have observed i) a decrease of the molecular weight which has limited effect on mechanical properties (Hopmann et al., 2015; Perega et al., 1996) , ii) an increase in the mobility of the polymer chain and iii) no change for the degree of crystallization. To improve the properties of recycled PLA, additives can be added during the mechanical recycling step. Additive can be a chain extender or an organic peroxide, which react with the PLA residues giving rise to cross-linking, branching or chain extension reactions (Beltran et al., 2019). To improve the mechanical properties of recycled PLA, Zhao et al. (2018) proposed to use polydopamine (PDA) as adhesion promotor. Mechanical properties of recycled PDA/PLA filaments obtained from extruded PDA coated PLA pellets and recycled PLA are summarized in the Table 6.

PLA degradation depends of few factors such as molecular weight, crystallinity, purity, temperature, pH, water permeability. But it is known that PLA rapidly degraded under composting conditions. The hydrolytic degradation products are totally assimilated by microorganisms.

The object manufactured by 3D printing presents poor interfacial strength at interfilamentous junctions. The mechanical properties of parts are as high as those of parts manufactured by injection molding.

Table 6 Mechanical properties of recycled PLA and Recycled PDA/PLA filaments (Zhao et al., 2018)

	Recycled PLA	PDA coated recycled PLA
Ultimate tensile stress (MPa)	46.35	53.24
Strain at break (%)	9.05	12.79

A solution to improve adhesion between two separated polymer surfaces is to use mending agent. Davidson et al. (2018) have proposed a furanmaleimide Diels Alder agent. While cross-section of pure PLA parts has shown a success of filaments layers with spaces at interfilamentous junction, remendable PLA has presented observable voids and interfilamentous boundaries.

To increase its mechanical performance, PLA can be reinforced with a particles or fibers. It exists a wide choice of reinforcements: metal particles, wood or plant fibers, beer, coffee or algae residues. PLA is a clear, colorless thermoplastic but it is offered for sale in various colors. There are more than 15 PLA filaments manufacturers and more than 500 references. Filaments are available unto several categories depending on diameter (1.75 mm or 2.85 mm), conditioning (0.5 to 6 kg), color (more than 10), translucence (zero, low medium and high), minimum extrusion temperature ([180-190°C] to [220-230°C]), durability (medium and high), rigidity (flexible to rigid) etc...

The most conventional printing conditions are summarized in the Table 7. Heated bed is not necessary for PLA printing. They can vary with manufacturers and product qualities.

Some like Volcano PLA of Formfutura ask for post-print annealing. It is design for high printing speeds up to 120 mm.s⁻¹. After extrusion, Volcano PLA has a high crystallinity content; it is rigid and temperature resistant. 3D printing temperature is recommended between 220 to 255°C and an annealing step is optional after annealing, the temperature resistance is up to 95°C.

Among the different commercial PLA filament, we find the LW-PLA of ColorFabb. This filament uses an active foaming technology which is triggered by temperature. At its peak, the filament will expand 3 x its volume. The filament density is variable. Before impression, density is in range of [1.21 – 1.43 g.cm⁻³] and after expansion, decreases in range of [0.403 – 0.476 g.cm⁻³]. The expansion will produce when temperature is around 230°C. it is necessary to decrease the printing speed, of 65%. Its leads to layer height important, until 0.6 mm with a nozzle of 0.4 mm. the manufacturer guidance indicates the stringing/oozing phenomena are inevitable.

Wood fiber or wood flour are the main reinforcement used but wood flour composites obtained by 3D printing have lower mechanical properties than those objects produced by traditional manufacturing processes (Auras et al., 2004). The incorporation of wood fibers in bio-composite reduces the cost of final products. In their study, Tao et al. have compared pure PLA and wood flour (WF)/ PLA composite with 5 %wt wood content (Wang et al., 2018). Before extrusion, PLA and WF were dried during 4h to eliminate the moisture. The device consisted in a single screw extruder with a maximum extrusion speed of 2 m.min⁻¹ for a diameter of 1.75 mm.

Table 7 3D printing commercial PLA filaments specifications

Density	1.2 - 1.45 g.cm ⁻³
3D printing temperature	180 – 220 °C
3D printing speed	40 – 100 mm.s ⁻¹
Heated bed temperature	20 – 60 °C

Both pure PLA and WF/PLA composite filaments were printed as test specimens with a self-assembled FDM 3D printer (603S model, Shenzhen Aurora Technology Co., Ltd., Shenzhen, China).

The nozzle diameter was 0.4 mm, and nozzle temperature was set at 210 °C during print. The addition of WF has changed the fraction surface: flat and smooth for pure PLA and rough for WF/PLA composite. Visible clusters of wood particles have been observed for higher wood content (Kariz et al., 2018). Without coupling agent, a poor interfacial bonding between PLA and WF has been observed. Glass transition and cold crystallization temperatures decreased with the addition of the wood flour, from 67 to 60°C and from 101 to 97°C respectively. On the other hand, the melting temperature of pure PA and WF/PLA composites were the same at 167°C. When strain was low (<1.5%) rigidity of wood flour/PLA composite was more important than pure PLA but for higher strains, it was the opposite. The 3D printed composite showed lower tensile mechanical properties. The same behavior was observed for cork/PLA composite (Daver et al., 2018). M. Kariz et al. (2018) studied too the impact of wood content on the mechanical properties. They used beech wood particles of 0.237 mm size and PLA matrix. Tensile strength increased from 55 MPa to 57 MPa with the addition of wood fibers from 0% to 10%. But beyond that, tensile strength decreased, until 30 MPa for 50% wood content. Commercial wood fiber filaments have higher wood fiber rates ranging from 10 to 40%wt (Le Duigou et al., 2016). Manufacturers announce that fibers adding does not change the printing condition. However, as Le Duigou et al. (2016) pointed out, mechanical properties are strongly dependant on printing orientation due to fiber anisotropy. Wood fiber orientation follows the printing orientation of the filament, weakening inter filament and interlayers interactions (Kariz et al., 2018). The printing width also influences the mechanical properties by changing the porosity of the printed object.

3.2.2 Butanediol Polyesters

The butanediol polyesters are promising biodegradable aliphatic polyesters. They are used in various forms such as films, packaging, injection-molded products and in biomedical applications (Bai et al., 2018). Among butanediol polyesters, let us note poly(butylene succinate) (PBS), poly(butylene adipate) (PBA) and poly(butylene succinate adipate) (PBSA). Poly(butylene succinate) (PBS) and its co polymers are synthesized via polycondensation of succinic acid and 1,4- butanediol. Generally, succinic acid is manufactured by hydrogenization of maleic anhydride. This one is itself obtained by oxidation of butane or benzene. It is the petroleum way (Fig. 16, Fig. 17). Since 2010, the biologic way from renewable feedstocks is developed and commercialized (Xu and Guo, 2010). Succinic acid can be then obtained from fermentation of microorganisms on glucose, starch, xylose... Most of the time, the production of 1,4-butanediol is from petroleum feedstocks. There exists an alternative from a biobased process. In the case, succinic acid is obtained from fermentation of renewable feedstocks such as corn-derived glucose or dextrose. After a purification by electrodialysis, succinic acid is reduced catalytically to 1,4- butanediol. Succinic acid and 1,4-butanediol are esterified to obtain oligomers which are polycondensed to remove 1,4-butanediol to form high molecular weight PBS. In the case of poly(butylene adipate) (PBA) 1,4-butanediol is esterified with adipic acid. PBS is soluble in various solvents: chloroform, dichloromethane, 1,1,1,3,3,3-hexafluoro-2-propanol, o-chlorobenzene.

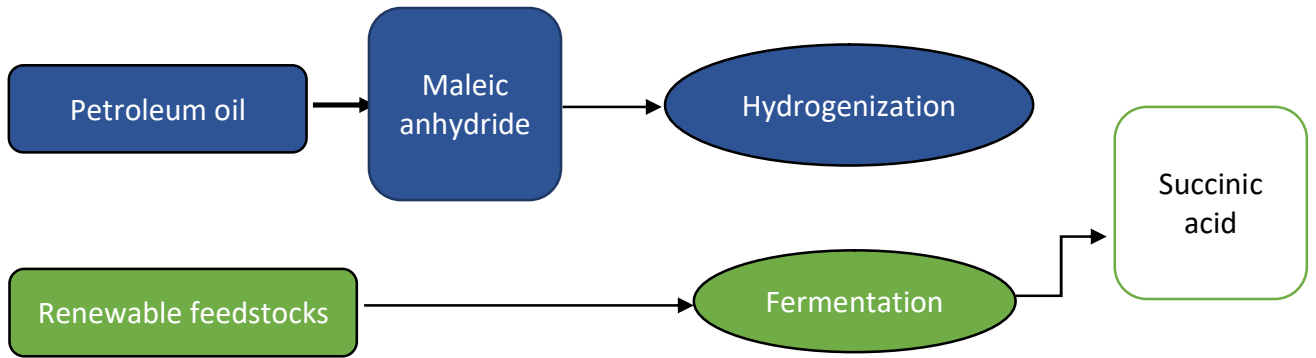


Fig 16. Synthesis of Succinic Acid.

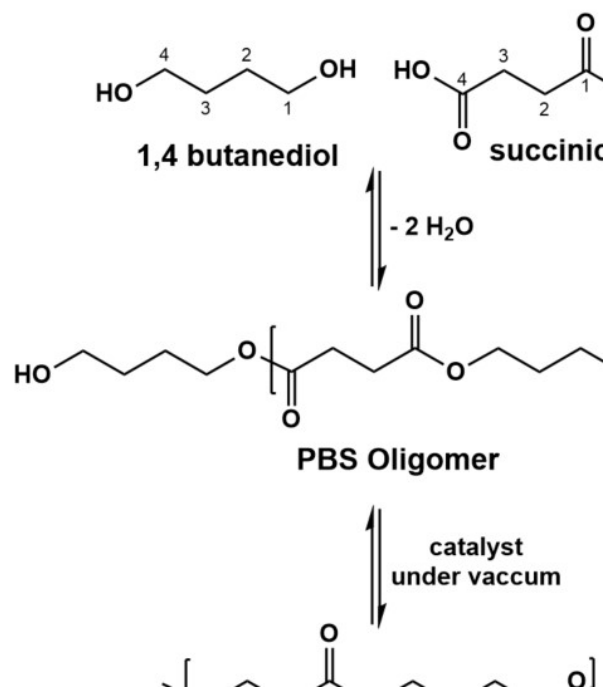


Fig 17. Synthesis of PBS from succinic acid and 1,4- butanediol.

Glass transition temperature of PBS is around of $-32\text{ }^\circ\text{C}$ and its melting point is $114\text{ }^\circ\text{C}$ (at peak). Properties of PBS depend of its molecular weight, but it is comparable to polypropylene. With high molecular weight, PBS is ductile since its elongation at break can reach 270% and its Izod impact strength $73\text{ J}\cdot\text{m}^{-1}$ (Xu and Guo, 2010). It can be used for blowing processes. But to be extruded or injection molded, PBS needs a molecular weight less than 100 000. In this case, PBS is brittle with an elongation at break around 10% and the Izod impact strength less than $40\text{ J}\cdot\text{m}^{-1}$. PBS is sensitive to water content. Before thermal processing (extrusion or printing) PBS pellets can be dried until a water content lower than 0.1 % to avoid hydrolysis at high temperature. Note that when processing temperature is upper that $200\text{ }^\circ\text{C}$, the shear viscosity decreases drastically (Xu and Guo, 2010). Melt flow rate (MFR) of PBS depends of the grade of PBS and its co-polymers. Properties of typical grades of bionolle® PBS are summarized in Table 8 (Rudnik, 2013).

Table 8 Properties of typical grades of bionolle® PBS (Rudnik, 2013)

Properties	Bionolle™ 1000 series (PBS)		Bionolle™ 3000 series (PBSA)	
	1001 MD	1020 MD	3001 MD	3020 MD
Density (g.cm ⁻³)	1.26		1.23	
Degree of crystallinity	35-45		20-35	
Melting point (°C)	114		94	
Glass transition temperature (°C)	-32		-45	
MFR (g/10min)	1-3	20-34	1-3	20-34

Table 9 Mechanical properties of PBS/PLA and PBSA/PLA blends bars obtained by injection molded (Xu et al., 2010)

	Elongation at break (%)	Tensile strength at yield (MPa)	Tensile strength at break (MPa)	Izod impact strength (J/m)
PBS	275±3.5	35±1	29±2	73±28
PLA/PBS 60/40	112±82	39±3	12±5	29±4
PLA/PBS 80/20	277±47	45±4	22±9	28±2
PBSA	476±124	30±1	28±3	132±32
PLA/PBSA 60/40	225±64	37±1	17±11	39±4
PLA/PBSA 80/20	319±17	49±1	23±8	24±2

Q. Ou-Yang et al. remarked that few studies are made on PBS because of the difficulty of forming monofilament (Ou-Yang, 2018)

PBS can be mixed with PLLA. The expected properties are tensile strength, elastic modulus, elongation at break and ductility. Xu et al. (2010) compared in their review mechanical properties of PBS/PLA and PBSA/PLA blends bars obtained by injection molded (Table 9). Poly(butylene succinate-co-butylene adipate) (PBSA) properties are function of the butylene adipate content. PBSA with 5-15 mol% butylene adipate content is interesting for its crystallinity and its tensile strength higher than those of PBS.

C. Boudouard et al have obtained PBS/PLLA 50/50 wt% composite obtained by injection and PBS/PLLA 50/50 wt% with 10% of flax fibers filaments. The comparison is interested to observe the loss of properties between composites obtained by injection and by 3D printing. Pellets of PBS/PLLA50/50 wt%- 10% of flax fibers were obtained in two steps to remove water. In a first step, formulations were compounded with a twin screw extruder at 190°C and 20 rpm. Extruded composites were the granulated and dried at 50°C. Some of them were injected to produce tensile specimens and the others were extruded using a single-screw extruder to produce the filament. 3D printer was equipped with a 1.0 mm nozzle and an extrusion temperature of 190°C. Printing speed was in range 0.8-1.5 m.min⁻¹ with a Z amplitude varied from 0.6-1.0 mm. Parameters used by Q. Ou-Yang et al. (2018) to print PBS/PLA material is summarized in Table 10.

Table 10 Parameters for 3D printing of PBS/PLA material in Q. Ou-Yang et al. study (2018)

Printing parameter	Amount
Temperature	200-230 °C
Speed	40 mm.s ⁻¹
Nozzle diameter	0.4 mm
Layer height	0.1 mm
Heated bed temperature	Room temperature

3.2.3. Polybutyrate adipate terephthalate (PBAT)

Polybutyrate adipate terephthalate (Fig 18) is synthesized from the polymer of adipic acid, 1,4 butanediol and the polymer of dimethyl terephthalate with 1,4 butanediol. It is a random co polymer known to be flexible and tough with a wide melting point. The random structure means that it cannot crystallize. Its density is 1.26 g.cm³. The glass transition of PBAT is -28 °C its melting temperature is in range of 110-120 °C (Table 11) whereas its VICTA temperature is 89°C). Its melting flow rate is more than 5g/10 min at 190°C and 2.16 kg.

PBAT is biodegradable: Zhao et al. have estimated its degradation around 90% after 80 days in testing (Zhao et al., 2010). PBAT is very interested to drastically improve the toughness of PLA. Notched impact strength of PLA increased from 5.1 kJ.m⁻² for pure PLA to 37.2 kJ.m⁻² for PLA with PBAT20wt%. With this PBAT content, PLA/PBAT blend elongation at break reached more than 600 %. S. Wang et al. are not so optimistic but they confirmed the increase of elongation at break: PLA/PBAT (80-20 wt%) printed bar obtained a strain at break in tensile mode of 38% versus a value of 4% for PLA printed bar (Wang et al. 2019). In the same time, the Young modulus was 2471 MPa for PLA/PBAT (80-20 wt%) printed bar versus 3282 MPa for PLA printed bar.

S. Singamneni et al. (2018) have realized successfully PBAT filament reinforced by wood flour in range of 0-20 wt%. They used a homemade extrusion 3D printer. 3D printing parameters are summarized on Table 12. Mechanical properties of 3D printed samples were significantly lower than that of injection molded samples. For example PBAT/woof flour (95-5 wt%) 3D printed samples have a strength of 53MPa and a flexural modulus of 403MPa while the same composition sample obtained by injection have a strength of 49MPa and a flexural modulus of 483MPa.

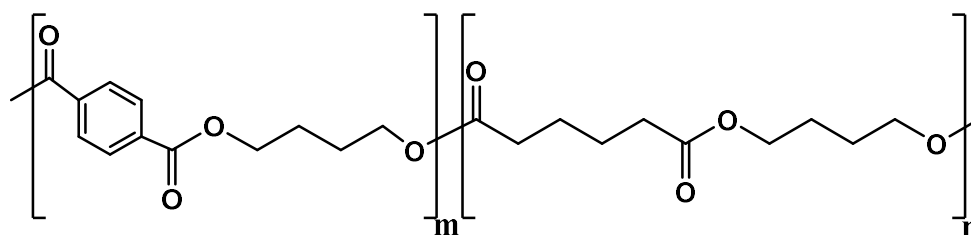
**Fig 18.** Structure of PBAT.

Table 11 Thermal characteristics of PBS, PBA and PBAT

polyester	Tg (°C)	Tm (°C)
PBS	-36	114
PBA	-68	55
PBAT	-28	114

Table 12 Printing parameters used by Singamneni et al. (2018)

Material	Extrusion Temp. (°C)	Bed Temp. (°C)	Spindle Velocity (RPM)	Print Velocity (mm/min)	Strand Gap (mm)
PBAT (100wt%)	120	110			
PBAT/ WF (95/5wt%)	135	110			
PBAT/ WF (90/10wt%)	130	110			
PBAT/ WF (80/20wt%)	140	110			

3-3 Polymers from microorganisms obtained by extraction (group 2): Polyhydroxyalcanoates (PHA)

Polyhydroxyalcanoates are accumulated biopolymers in bacterial cells in the form of granules. This accumulation is caused by the lack of a nutrient in the presence of an excess of carbon substrate. PHAs can be produced by a large number of microorganisms for energy storage purposes. Chemical nature and characteristics of PHAs are dependant of culture conditions, carbon substrate and selection of bacterial species. Menčík et al. (2018) announced the number of 150 different PLA monomers (Table 13).

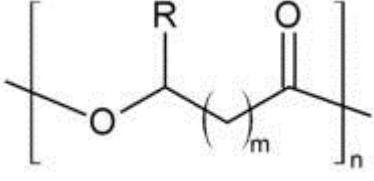
Polyhydroxyalcanoates can be divided into 3 categories: i) short chain length (scl) PHA constituted of hydroxyalcanoic acid with a maximum of 5 atoms; ii) medium chain length (mcl) PHA which monomeric units are in range of 6-12 atoms and iii) long chain length (lcl) PHA with 12- 16 atoms. Short chain length PHAs are rigid and brittle and they are considered as thermoplastics. Mcl et lcl PHAs are considered as elastomers and adhesives.

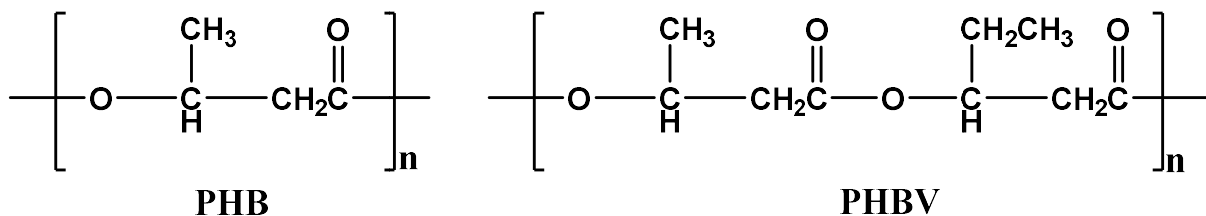
Poly(3-hydroxybutyrate) PHB and poly(3-hydroxybutyrate-co-3hydroxyvalerates) PHBVs are the most common family members of PHAs (Fig. 19). Poly(3-hydroxybutyrate) is a linear saturated polyester. PHBV is obtained by copolymerization with hydroxyvalerate (HV). PHB and its co polymers PHBV are biodegradable and biocompatible but they present a poor thermostability and a relatively low impact resistance (Avella et al., 2000). PHBs are insoluble in water, but they are soluble in almost apolar solvent, such as chloroform.

PHB is a semi crystalline polymer with high melting temperature (170°C) and high degree of crystallinity (80%) (Menčík et al., 2018; Vaidya et al., 2019). Glass transition temperature is sometime no discernible (Vaidya et al., 2019; Zhang et al., 2011). PHBV is more ductile than PHB, with lower melting point and lower strength and rigidity. The melt flow rate of PHB (NaturePlast, France) is estimated to 15-30 g/10min tested at 210°C and 2.16kg loading (Armentano et al., 2015).

PHA filaments for fused deposition modeling are generally added with natural fibers (Chiulan et al., 2018). To increase the interfacial adhesion between PHA and fibers, a fiber treatment is used with a coupling agent or a reactive compatibilizer (Anderson et al., 2013)[.

Table 13 Various types of PHA and PLA

	m value	R nature	PHA type
	m = 0	R=CH ₃	Poly(lactic acid (PLA))
	m = 1	R=H	Poly(3-hydroxypropionate) (PHP)
	m = 1	R=CH ₃	Poly(3-hydroxybutyrate) (PHB)
	m = 1	R=C ₂ H ₅	Poly(3-hydroxyvalerate) (PHV)
	m = 1	R=C ₂ H ₇	Poly(3-hydroxyhexanoate) (PHH)

**Fig 19.** Chemical structure of PHB and PHBV.

Silane or acylation are used a coupling agent. Silane coupling is tetrathoxysilane (TEOS) (Wu et al., 2017). For acylation of the hydrophilic hydroxyls, Shibata et al have selected butyric because the carbon number of the acid components in ester groups of PHBV is the same than those of treated fibers (Shibata et al., 2002). Maleated polymer are used as reactive compatibilizer. Effectiveness of maleic anhydride grafted PHBV (PHBV-g-MA) was shown in various studies (Anderson et al., 2013; Wu and Lioa, 2017). Wu et al. (2017) have made a PHBV-g-MA/palm fiber filament. Tensile strength was 7 MPa and Young modulus was 65 MPa with 20 wt% incorporation of fibers (Wu et al., 2017). They have concluded than the prepared palm fiber-reinforced polyhydroxyalkanoate is a good candidate for 3D printing filament, due to its low cast and excellent characteristic.

In general, commercial PHA filaments are mixed with PLA. For some authors, PLA and PHA are immiscible but they exhibit molecular interactions (Zhang and Thomas, 2011) For some others, PHB is miscible with low molecular weight PLA ($M_w < 18000$) but for high molecular weight PLA, PHB/PLA blends present biphasic separation (Koyama and Doi, 1997). When PHB is the major phase, PLA is miscible with low molecular weight ($M_w < 9400$) and immiscible with high molecular weight PHB. To increase the compatibility between PHB and PLA, compatibilizers can be used: glycidyl methacrylate, poly(ethylene glycol) or poly(vinyl acetate) (Abdelwahab et al., 2012).

In PHB/PLA blends, PHB particles are disperse as fillers in PLA, which should improve the mechanical properties. In their study, Zhang and Thomas have observed than glass transition

temperature of PHB/PLA blend is always 5°C below PLA glass transition temperature (i.e. 50°C instead of 55°C for pure PLA) (Zhang and Thomas, 2011). Whatever PHB/PLA ratio, blends have presented brittle fracture. Both tensile stress at break and elongation at break have decreased with the PHB content. However, the PHB/PLA 25/75 blend has presented better mechanical properties than pure PLA. Tensile strength at break has reached 32 MPa with an elongation near 17%. The thermal history of the PHB/PLA blend is also important. Zhang et Thomas (2011) have compared mechanical properties of quenched and annealed PHB/PLA 25/75 blends. After dynamic mechanical analysis, they have concluded that annealed PHB/PLA 25/75 blend showed better mechanical properties and higher thermal distortion temperature than quenched PHB/PLA 25/75 blends.

To improve the mechanical properties of PHB/PLA filament, a solution is to add a plasticizer. Some of them lower the glass transition temperature and increase the elongation of the polymer. A comparison is made between a polyester-type plasticizer (lapol108) and citrate plasticizers. Abdelwahab et al. (2012) have compared mechanical properties of pure PHB and PHB with lapol 108. Their results are summarized in Table 14. They have tested with PHB/PLA blends with PHB/PLA ratio of 25/75.

Menčík et al. (2018) have compared another type of plasticizers based on esters of citric acid. The best results were obtained with tributyl citrate (C-4) and acetyl tributyl citrate (A-4) as plasticizers with an improvement of ductile properties. However, it is interesting to note a decrease of the elastic properties of plasticized PHB/PLA filaments after 40 days. Printing has modified the mechanical properties of the initial filaments (Table 15) with a lower elongation at break.

Before printing, it is necessary to dried the filament. Balogová et al. (2018) have compared dried and undried PHB/PLA 25/75 blends during and after printing. Parameters of 3D printing are summarized in Table 16. Undried material showed high variable viscosity values compared to dried material.

Table 14 Mechanical properties of pure PHB and PHB/Lapol 108 (Abdelwahab et al., 2012)

	Pure PHB	PHB /Lapol 108 (5wt%)
Young Modulus (MPa)	1950	1750
Tensile strength (MPa)	31	29
Elongation (%)	7.2	7.2

Table 15 Young's modulus (E) and Tensile Strength (TS) of PHB/PLA and PLA/PHB/plasticizer samples. 3D printing was executed approximatively 6 months after the filaments preparation (Menčík et al., 2018)

Samples		Filaments - 7 days after preparation	Filaments-40 days after preparation	Printing object – 7 days after printing
PHB/PLA (70/30)	E (GPa)	0.57±0.07	0.45±0.12	2.41±0.13
	TS (MPa)	43.31.0	42.9±1.9	39.1±1.6
PHB/PLA /C4 (60/25/15)	E (GPa)	0.16±0.01	0.17±0.00	0.66±0.05
	TS (MPa)	19.5±0.5	20.2±0.8	19.8±0.3
PHB/PLA /A4 (60/25/15)	E (GPa)	0.15±0.01	0.17±0.01	0.69±0.02
	TS (MPa)	20.1±0.9	22.5±0.4	22.1±1.0

They concluded that, after drying at 80°C during 60 min, the PHB/PLA filament was more stable during printing. The printed object was degraded much less quickly than the one made with an undried filament.

PHB can also be mixed with PCL. PHB and PCL are considered as immiscible in the melt and the amorphous state (Kumagai and Doi, 1992). It is possible than a small amount of solubilization from one to this other occurs. For 60% PLC content and above; PLC forms a continuous matrix with PHB spherulites embedded it. For less than 60% PCL, PHB forms a continuous phase (Avella et al., 2000). In both cases, the mechanical properties are closed to the continuous phase. Kumagai et al. (1992) have studied the properties of PHB/PCL blends films. They observed two glass transition temperatures that confirmed PHB and PCL are not miscible. They have concluded than the mechanical properties of PHB/PCL blend films decreased with the increased of PCL ratio until 50 wt% (Table 17). Above 50 wt% PCL ratio, mechanical properties increased with the increased of PCL ratio. To increase the miscibility between PHB and PCL, the two polymers can be melted mixed by adding peroxide. Dibenzoylperoxide (DBPO) or dicumylperoxide (DCPO) can be used (Avella et al., 2000).

Table 16 Parameters for 3D printing of PHB/PLA material in Balogová et al. study (2018)

Printing parameter	Amount
Temperature	180-230 °C
Pressure	5 Bars
Speed	3 mm.s ⁻¹
Interval	10 minutes
Nozzle diameter	0.6 mm
Needle offset	0.48
Volume of high temperature cartridge	4 g

Table 17 Thermal and mechanical properties of PHB/PLC blend films (Kumagai and Doi, 1992)

PHB/PCL Blend composition (wt% ratio)	Tg (°C)	PHB Tm	PCL Tm	Young's modulus (MPa)	Tensile strength (MPa)	Elongation at break (%)
100/0	1	179	-	1560	38	5
77/23	4	178	59	730	21	9
49/51	2	178	59	110	4	18
25/75	1	178	60	220	8	11
0/100	-70	-	60	220	15	24

3-4 Polymers from biomass (group 1)

3.4.1 Starch (TPS)

Starch is a complex natural polymer. It presents naturally in plant tissues, in form of water-insoluble granules. The granules contain ordered region which are semi-crystalline and the granules sizes are ranging from 1 to 100 µm. It consists to a mixture of two homologous

polysaccharides, amylose and amylopectin (Fig. 20), in various proportions depending of the plant origin (Keetels et al., 1996; Nessi et al., 2018). Amylopectin is the main component whose short chains are organized into double helices to form crystallites. Amylose is an essentially linear molecule consisting of (1-4)- α -linked D-glucan chains. Amylopectin is a highly branched molecule. It contains short chains of 1-4)- α -linked D-glucan with (1-6)- α -linked branches. Content of amylose and amylopectin depends of the starch origin.

For native starch, thermal degradation occurs before melting, which prevents its direct implementation by melt-process. The melting temperature of pure dry starch is 220-240°C and its decomposition starts at 220°C. Native starch is converted into TPS under heat and shear in the presence of plasticizers (Fig. 21) (Ghanbari et al., 2018). Plasticizers interact with the hydroxyl groups of starch that means to a reduction of hydrogen bonding among the starch. So, the melting temperature of starch is lower than the degradation temperature. The formed thermoplastic starch can be melt processed with conventional technologies (extrusion and injection-molding). Used plasticizers are polyols (glycerol, sorbitol, polyethylene glycol) or nitrogen compounds (urea, amines, ammonium derived) (Mitrus, 2009). Water is often added as a destructuring agent and a volatile plasticizer (Av erou and Halley, 2009). The combination of heat and water leads to the gelatinization of starch that lead to the disruption of the highly granular organization and the starch swells. A viscous paste is forming with destruction of most of hydrogen links. Melting and glass transition temperature are reduced.

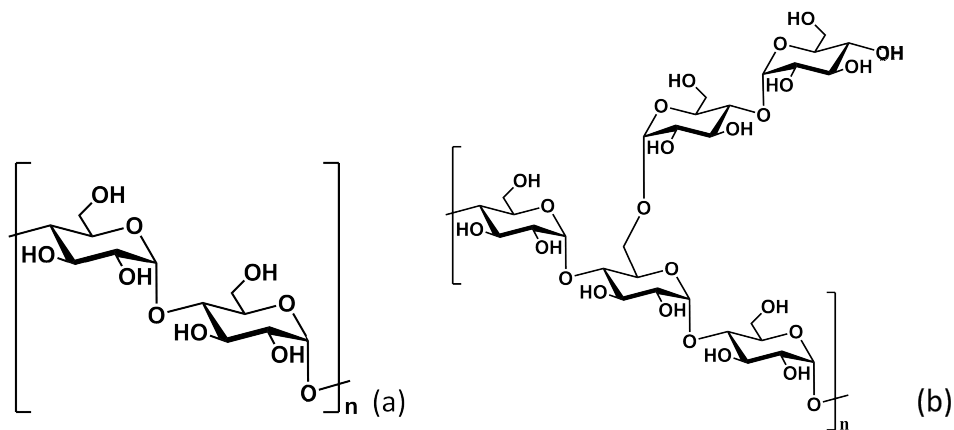


Fig 20. Structure of amylose (a) and amylopectin (b).

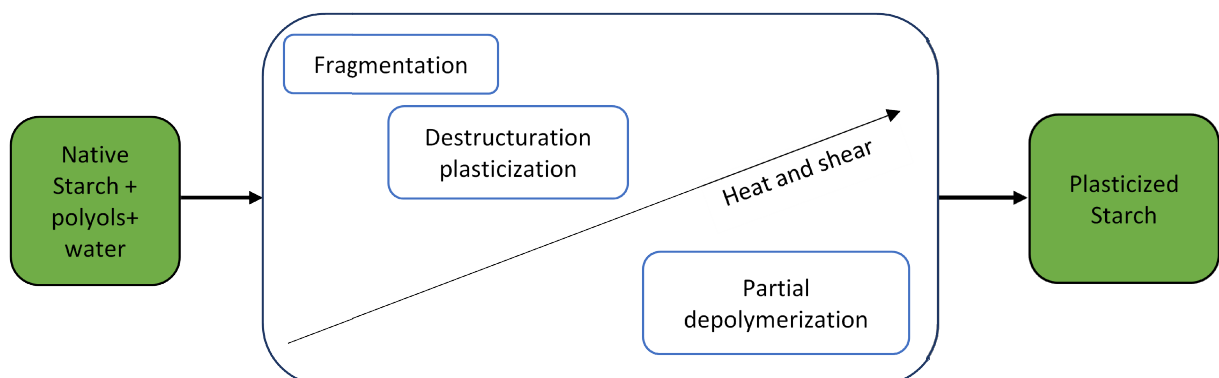


Fig 21. Schematic transformation of native starch to thermoplastic starch.

Table 18 Thermal and physical properties of plasticized starches in function of glycerol and water contents (Avérou and Halley, 2009)

Initial formulation	Glycerol/dry starch ratio (wt/wt)	Water (wt%)	Density	Tg (°C)	α transition (°C)	Modulus (MPa)	Max tensile strength (MPa)	Elongation at break (%)
S74G10W10	0.14	9	1.39	43	63	1144	21.4	3
S75G18W12	0.25	9	1.37	8	31	116	4.0	104
S67G24W9	0.35	12	1.35	-7	17	45	3.3	98
S65G35W0	0.50	13	1.34	-20	1	11	1.4	60

Properties of TPS depend of the plasticizer/starch ratio. Avérou et Halley (2009) have presented the impact of glycerol and water contents on glass transition temperature and mechanical properties of plasticized starches (Table 18). Three types of starches (potato, rice and corn) were studied in the aim to evaluate their rheological properties and their printability (Chen et al., 2019). Their amylose content and moisture are summarized in the Table 19. Steady shear rheological measurements were conducted. The conclusion was rice starch was much rigid than potato and corn starches and would show a gelling behavior during the heating. Gelling behavior is critical for the printing medium to be dispensed as a free-standing filament so, rice starch was more preferable as printing medium. However, the three types of starches are printable according to the conditions summarized in Table 19. They have excellent printability, shape retention and resolution.

The chemical structure of starch is composed of numerous hydroxyl group (OH) which is referred to as a hydrophilic group, so the thermoplastic starch is more sensitive to water in ambient condition and lose its properties. Ageing of TPS depends of the temperature. At temperature inferior to glass transition temperature, physical ageing occurs versus time and TPS presents a densification. At a temperature above Tg, retrogradation phenomena modify the crystallinity and plasticizer molecules rearrangements (Avérou and Halley, 2009). To reduce hydrophilic character of TPS, structure of starch can be modified by acetylation but it leads to lower mechanical properties. Another solution is mixing plasticizer starch with another biopolymer: PCL, PLA, PHBV [Avérou et al., 2000, Kalambur and Rizvi, 2006].

Table 19 Amylose and moisture contents of corn starch, potato starch and rice starch and conditions of printing (concentrations and printing temperature)

	Amylose content	Moisture (%)	Concentrations %(w/w)	Printing Temperature (°C)
Corn starch	24.1±0.6	14.59±0.01	20-25	75
Potato starch	34.5 ±0.4	15.54±0.03	15-20	70
Rice starch	26.5±0.3	14.97±0.05	15-25	80

3.4.2 Cellulose

Cellulose is the most abundant renewable biopolymer on Earth. It is the main structural component of plant cell wall (35 to 50%). Cellulose consists of a repetition of β -D-glucopyranose units (Fig. 22), that are covalently linking through acetal function between the C1 carbon atom and the equatorial -OH group of C4 (Dai et al., 2019). Cellulose is insoluble in water and in common organic solvents due to the preferential formation of intra- and intermolecular hydrogen bond (Peng et al., 2017). The manufacturing of cellulose is done in several steps. The first step is the separation between cellulose and hemicellulose/lignin by dissolution. Cellulose is infeasible for extrusion because its degradation temperature is inferior of its melting temperature (Wang et al., 2018). Cellulose glass transition temperature is in range of 200 – 230°C and thermal degradation starts 260°C (Oksman et al., 2016). However, nanocellulose hydrogels showing a shear-thinning behavior might be considered as extrudable precursors for 3D printing. Cellulose is promising ink which focuses on pharmaceutical products and biomedical devices. Its characteristics are excellent such as low density, biodegradability, ecofriendliness, toxicological harmlessness.

Other characteristics are high specific stiffness, good thermal and acoustical insulation. For these reasons, lignocellulose materials were mainly used as reinforcement component to improve the mechanical properties. The hydrophilicity and less thermal stability of cellulose micro/nanoparticles restrict the range of choice of polymer matrix [Oksman et al., 2016]. The mechanical properties of PLA, PCL and PA were modified using cellulosic fibers (Bai et al., 2013). For example, Murphy and Collins have used microcrystalline cellulose (MCC) as reinforcement in PLA 3D printing composites (Murphy and Collins, 2016). MCC was surface modified using a titanate coupling agent (Lica 38) to improve its compatibility with PLA matrix. Only 3wt% of MCC increased significantly the crystallinity and the storage modulus of the composite.

Low amount of nanocellulose is used, about 1-5% as reinforcement phase. The process for nanocellulosic preparation is complex and expensive, so the application of such composites is still restricted [(Wang et al., 2017). However, Wang et al. have shown that it is possible to add until 30% of cellulose fibers in a PLA matrix using a mixing of micro and nano cellulose. To increase the interface compatibility between cellulose and PLA, silane (KH550) was used as a coupling agent (1%). Incorporation of PolyEthylene Glycol (PEG) in PLA increased the chain mobility and improved the elongation at break. For mixture of 30% cellulose, 65%PLA and 5% PEG, elongation at break was 12%, tensile strength was 59.7 MPA and flexural strength was reached 50 MPa.

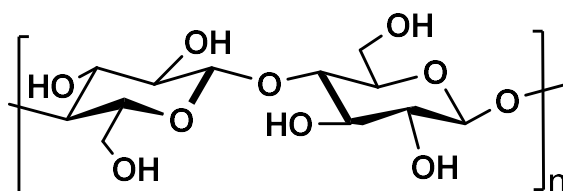


Fig. 22 Structure of cellulose

Table 20 Physical and thermal properties of cellulose acetate (Tag3D FilAcetate)

Density (g.cm ⁻³)	1.27
Glass transition temperature (°C)	70
Melting point (°C)	200

Cellulose can be chemically modified to obtain a thermoplastic. The best transformation is esterification rather than etherification. The most common cellulose esters in this field are cellulose acetate (CA), cellulose acetate propionate (CAP) cellulose butyrate (CAB), nitrocellulose (Dai et al., 2019). Its hypoallergenic properties and its mold resistance make it possible prints parts that will be in contact with the skin. Cellulose acetate is natural resistance to UV and to chemical agents such as chlorine. Its properties are summarized in Table 20. Cellulose acetate has an excellent print quality with or without hot bed and presents no shrinkage and warping. During the print, acetate evaporates but some advice to immerge the final piece in a sodium hydroxide to remove the acetate and restore the cellulose with its full network of hydrogen bonds (www.sculpteo.com/blog/2018/12/12/faster-3d-printer-and-antibacterials-3d-printed-cellulose-mit-is-going-further/).

Paggi et al. (2019) have studied the influence of printing parameters on mechanical properties of the piece (Table 21). They used corn starch/cellulose acetate (SCA blend 50/50 wt%, Mater-Bi® Y1010). Filament was produced by hot melt extrusion with a single screw extruder. The optimum conditions were: extrusion temperature 175°C, 60 rpm.

Table 21 Mechanical properties of SCA specimen 3D printed under different conditions of nozzle temperature of nozzle temperature and flow rate (Paggi et al., 2019)

Nozzle temperature	Flow rate	Flexural modulus (MPa)	Stress at 10% (MPa)
230	2.16 mm ³ .s ⁻¹	437.72 ± 44.76	41.19 ± 6.7
230	2.43 mm ³ .s ⁻¹	431.00 ± 38.03	48.13 ± 6.18
240	2.16 mm ³ .s ⁻¹	475.53 ± 4.04	53.61 ± 9.57
240	2.43 mm ³ .s ⁻¹	428.10 ± 19.87	40.74 ± 10.72

Nozzle size: 0.6 mm, layer height: 0.15 mm, print speed: 30 mm.s⁻¹

3.4.3 Lignin

Lignin is a biopolymer commonly found in plant cell walls linked to carbohydrates. It is the second most abundant macromolecule on Earth's surface after cellulose. Natural lignin extraction according different processes can give technical lignins with specific Mw, structure, and properties. The pulp and paper industry makes use of the cellulose fraction leaving lignin behind as a by-product with low-value. Today, although lignin raises scientists' interest for a wide range of applications, only 2 % of industrial lignin is valorized. Yet, with its high carbon content and its variety of functional groups (aromatic rings, methoxy, hydroxyl, etc.), lignin has the potential to substitute to some fossil-based materials, therefore playing a key-role in the development of environmental-friendly products.

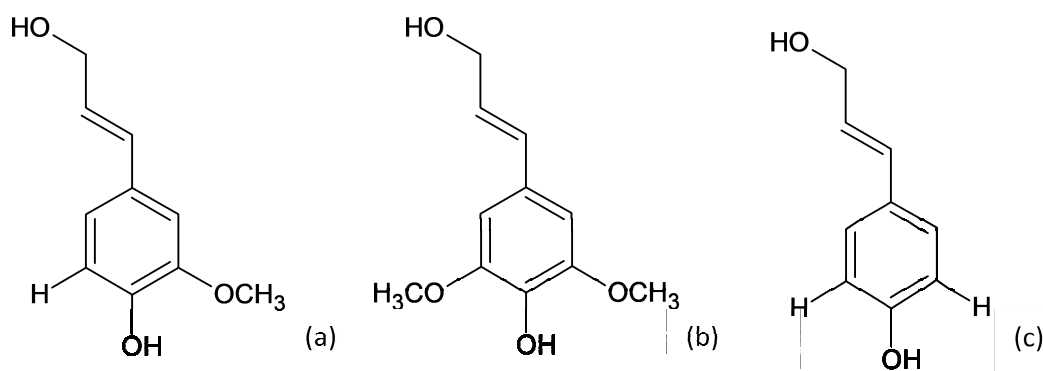


Fig. 23 Structure of p-coumaryl alcohol (a), coniferyl alcohol (b) and sinapyl alcohol (c)

One acknowledged obstacle to valorization is lignin's complex and heterogeneous structure.

Lignin is formed by the polymerization of 3 oxidized monolignols, ie. p-coumaryl alcohol, coniferyl alcohol, and sinapyl alcohol (Fig. 23) giving rise to a variety of linkages. Ether linkages such as β -O-4 linkage which is present in larger quantity are mainly cleaved during extraction.

Some achievements can be reported for 3D-printing of lignin. The main limitations are difficulties in melt processing the lignins (Nguyen et al., 2018a), their brittle behavior, or a rough surface of the filament when used as a filler (Ghartzou et al., 2017). Extrusion of lignin fibers is possible from swollen gels or melts. The main application is the preparation of carbon fibers from lignin fibers. Some apparatus such as Xplore Instruments BV lignin extrusion line were developed especially for extruding lignin fibers. In this process, lignin monofilaments can be crosslinked for a further conversion to carbon fibers by pyrolysis (<http://www.xplore-together.com/products/lignin-line/about-micro-fiber-line-copy>).

Lignin was not used as a mono-constituent for 3D-printing. But when blending it with other polymers, melt processing difficulties were overcome. Addition of fibers could enhance 3D-printed specimens' stiffness. Lignin is known as anti-oxidant (free radical scavenger) and fire retardant. The use of lignin fillers in 3D printing would have the potential to reduce flammability and preserve the filaments from oxidation. An interesting fact for 3D-printing market is the reduction of filaments cost since lignin is a very cheap and abundant raw material.

To improve melting of the filaments for 3D-printing, lignin was blended or formulated with other thermoplastic polymers. Fused filament fabrication (FFF) process is generally used. Some processing parameters of different studies are presented in Table 22. Materials made of lignin plus poly(lactic acid) (PLA) or polyhydroxybutyrate (PHB) are bio-based and biodegradable. Materials made of lignin plus polyolefins or acrylonitrile-butadiene-styrene (ABS) are not biodegradable.

Blending lignin with PLA gives possibilities in the area of 3D-printing. Obtaining homogeneous filaments could sometimes be challenging since a good compatibility between lignin and PLA was not always exhibited. Gkartzou et al. observed Kraft lignin aggregation when 3D-printing specimens [128].

Table 22 Review of several processing parameters / characteristics

Reference	Extrusion temperature (°C)	Nozzle temperature (°C)	Printing speed (mm/s)	Nozzle diameter (mm)	Filament diameter (mm)
Ghartzou et al., 2017	180 - 190	205	20	0.2 - 0.3 - 0.4	1.78
Obielodan et al., 2018	170 - 175	190 - 210	-	-	1.77
Domínguez-Robles et al., 2019	170 - 190	185 - 205	-	0.4	2.85
Vaidya et al., 2019	160 - 170	190	25	-	-
Shao et al., 2018	-	-	9	0.5	0.6
Nguyen et al., 2018b	210	230	50	0.5	2.5

Observation of lignin-PLA interface by SEM showed a separation between lignin's aggregates and the PLA matrix. This resulted in nozzle clogging for highest lignin loading and in roughness of the filament's surface compared to pure PLA.

Therefore, the blend containing 5 wt.% Kraft lignin was recommended for 3D-printing (Ghartzou et al., 2017). The authors suggest that lignin could affect nucleation and crystal growth in the PLA phase with the formation of thicker crystalline structures during PLA cold crystallization. *3R3D Technology Materials* developed its Lignina® product made of PLA with 10 wt.% micronized lignin powder showing in this case, a smooth filament's surface (<https://www.3r3dtm.com/producto/lignina-filamento-3d-175-mm-0-75-kg>). FPinnovations investigated the use of a coupling agent to improve lignin-PLA homogeneity by chemically bonding them (Li et al., 2019). The authors exposed that they could reduce agglomeration of lignin particles allowing the fabrication of 3D-printed specimens that contain up to 20 wt.% lignin. Lignin addition did not impact tensile strength properties. Obielodan et al. claimed that they successfully filled a PLA matrix with organosolv lignin up to 25 wt.%. With organosolv lignin, no agglomeration effect was observed. Very good processability of the blend as well as smooth surface of the extruded filament were reported (Obielodan et al., 2018). As for Ghartzou et al. (2017) tensile strength of specimens containing lignin decreased. Contrary to Kraft lignin, organosolv lignin improved the material's ductility. With Kraft lignin a decrease of elongation at break and a brittle behavior was reported. Domínguez-Robles et al. (2019) used a coating method on PLA pellets with castor oil so that they could add 0.5 to 3 wt.% lignosulfonates powder on the surface. The goal of this study was to highlight antioxidant properties brought by lignosulfonates for biomedical purpose. Extrusion and 3D-printing of such material was demonstrated.

Lignin could also be used as filler in biodegradable polyesters such as PHB (polyhydroxybutyrate). Scientists of *Scion* research institute produced filaments that contained up to 20 wt.% biorefinery lignin produced by the enzymatic saccharification of pretreated *Pinus radiata* pulp in a PHB matrix (Vaidya et al., 2019). Lignin addition induced a melt rheology suitable for 3D-printing, especially for 20 wt.% lignin ratio. The authors noted

after FTIR and SEM analyses that lignin particles are more likely to be present in the filament core rather than in the surface that is PHB rich. Thermal analyses assessed that lignin acted as non-reacting filler. Yet, reduced shrinkage of printed specimens and better inter-layers adhesion were highlighted in the presence of lignin compared to neat PHB. Consequently, warpage was also reduced in the presence of lignin-filler, making 3D-printing much more convenient. Shrinkage moderation could be explained by the formation of micro-voids in the microstructure that reflects interfacial incompatibility between lignin and PHB.

Nguyen et al.(2019) prepared composites with lignin and polypropylene (PP) or polyethylene (PE) matrix. They investigated the influence of lignin on 3D-printing, melt-spinning, and mechanical performances of the composites. It was observed that amorphous lignin chains were aligned between PP and PE crystalline zones and that PP and PE crystallization rate was moderated in the presence of lignin.

Some materials containing lignin and fibers were developed. Natural fibers are often used for reinforcing 3D-printed materials. They are hydrophilic and relatively cheap but sensitive to temperature changes. Natural fibers confer a wood-like appearance to the product, especially when combined with lignin. Carbon fibers can also be added when high mechanical performances are looked for.

The German company *Tecnar* launched more than 3,500 composite products containing lignin and natural fibers under the tradenames ARBOBLEND[®], ARBOFILL[®], and ARBOFORM[®]. All the formula can be processed by injection-molding, and some of them can be 3D-printed(<https://www.tecnaro.de>). ARBOFORM[®] materials are especially filled in lignin. They exhibit a thermoplastic behavior as well as potentially interesting melt characteristics towards printing (Nägele et al., 2002; Nedelcu et al., 2013). Mechanical, thermal, and rheological properties of typical materials are reported in Table 23.

The company *Extrudr* provides filaments made of lignin, natural fibers, and other thermoplastic polymer under the trade name extrudr Wood[®] dark or nature which properties are reported in Table 23 (https://www.extrudr.com/en/products/catalogue/fichte-natur_2263/).

Shao et al. published a study on the fabrication of carbon-based electrodes composed of microfibrillated cellulose, lignosulfonate, and cellulose powder. A relatively high amount of lignosulfonates, i.e. 49 wt.% of the whole composition, was therefore valorized. The hydrogels were 3D-printed, and pyrolyzed to give a material with high electrical conductivity (Shao et al., 2018). A good adhesion between layers was obtained. After pyrolysis, cross-sections of the materials revealed porosities of various diameters up to 50 μm resulting in a low-density of 0.74 g / cm³. Mechanical properties remained interesting with an elastic modulus of 6.6 GPa for the sample submitted to a 900°C temperature.

Researchers of Oak Ridge Laboratory successfully 3D-printed a material containing up to 40 wt.% organosolv hardwood lignin (Nguyen et al., 2018b). They made use of acrylonitrile-butadiene-styrene (ABS) polymer matrix with its well-known properties suitable for 3D-printing. Hydrogen bonding between lignin and ABS was reported improving interfaces quality. At high lignin loading composites were relatively brittle with an ultimate tensile strain of 1.2% (Nguyen et al., 2018c). The authors believed that low molecular weight lignins enhance the brittleness in ABS matrix. They also tried to explain stiffness variations at macro-scale by the difference in lignin structure / functional groups. Rigid segments like biphenyl and biphenyl ethers of Kraft softwood lignin increased the thermal transition temperature causing a flow resistance detrimental to 3D-printing (Nguyen et al., 2018a).

These phenolic units also provided stiffness enhancement of the composites. On the contrary, aliphatic ether groups, aliphatic chains, and β -O-4 linkages within hardwood lignin favored the 3D-printing characteristics. In order to reduce the composites brittleness, acrylonitrile butadiene rubber (NBR) compatibilizer was added to the mix. Hydrogen bonding as well as covalent bonding were formed between lignin hydroxyl groups and NBR nitrile groups (Nguyen et al., 2017). The authors explained that free radicals from the less stable groups may form at high temperatures in the one-pot mix allowing the formation of new covalent bonds. Plasticity was enhanced thanks to NBR, therefore it was possible to add up to 40 wt.% lignin. Because of their intrinsic properties, carbon fibers reinforced the composite but they also acted as bridges between printed layers. Finally, carbon fibers may breakdown lignin particles during the mixing preparation step. Thus, carbon fibers contributed to a better adhesion of consecutive printed layers. The overall material exhibited strong mechanical performances with tensile strengths up to 65 MPa and elastic modulus of 2.6 GPa. Printing parameters are presented in Table 22.

Other materials with excellent 3D-printability were developed by mixing hardwood lignin with nylon 12 (Nguyen et al., 2018a). The dispersed lignin particles reduced the melt viscosity, improving the flow characteristics of nylon. Material containing 12 wt.% carbon fibers and 40 wt.% lignin had a tensile strength over 80 MPa and a tensile modulus of 6 GPa. Mixtures containing up to 60 wt.% lignin were 3D-printed.

Table 23 Properties of extruder Wood®, ARBOFORM®, ARBOBLEND®, and ARBOFILL® materials.

(¹): <https://www.tecnaro.de>; (²): <https://www.extrudr.com/en/products/catalogue/fichte-natur-2263/>

		ARBOFORM® (1)	ARBOBLEND® (1)[ARBOBLEND® (1)[ARBOFILL® (1)	Extrudr Wood® (2)
Mechanical properties	Tensile modulus (MPa)	6000	4800	2200	3100	3200
	Tensile strength (MPa)	15	55	45	33	40
	Strain (%)	0.3	2	4.5	3.5	-
	Tensile stress at break (MPa)	15	51	20	32	-
	Tensile strain at break (%)	0.3	4	18.7	4.1	2
	Flexural stress (MPa)	42	-	-	-	43
	Charpy impact strength (kJ / m ²)	2	51	130	-	-
	Ball indentation hardness (MPa)	122	-	-	-	-
Thermal properties	Linear expansion coefficient (K ⁻¹)	1.8.10 ⁻⁵	-	-	-	-
	Vicat temperature (°C)	83	-	-	-	48
	Heat conductivity (W/m/K)	0.384	-	-	-	-
Rheological properties	MVR (cm ³ /10 min)	-	8	32	6	-
	MFR (g / 10 min)	-	-	-	-	22
Others	Shrinkage (%)	0.2	2	-	-	-
	Density (g / cm ³)	1.29	-	-	1.03	1.23
	Water content (%)	6	-	-	-	-

3.4.4 Chitosan

Chitosan (CS) is a polysaccharide made up with two different monomers N-acetylglucosamine and glucosamine linked through β -1,4-glycosidic bonds (Fig. 24) (Brasselet et al., 2019). This polysaccharide is derived from another polysaccharide named chitin which is one of most earth abundant polysaccharide after cellulose. Chitin is present in a huge range of living organisms like lobsters, shrimps but also insects and fungi. Two main allomorphic forms of chitin exist, α and β -chitin. A third form γ -chitin which is a combination of α and β -chitin (Kaya et al., 2015). Chitin is insoluble in water or other common solvents however it can be converted into CS under hot and alkaline conditions. After this treatment, chitosan became soluble in slightly acidic medium which allows its formatting and its modification more easily. Chitosan and chitosan derivatives have many applications, one of the most promising opportunities is its use as biomaterial for production of tissues, skin and other materials. Several studies have shown that it's possible to use chitosan inks for bio 3D printing. Wu et al. have shown in their study that it was possible to produce chitosan inks adapted for 3D printing (Wu et al., 2018). In this case, production of chitosan inks was made up by dissolving chitosan in an acidic medium composed of 40% acetic acid, 40% water and 20% lactic acid, with various chitosan concentrations from 6 to 10 % wt. After centrifugation at 3000 rpm to remove air bubbles CS solution was placed into printer cartridge and extruded through 3D printer micronozzles of 150 μm at a speed of 1 to 2 mm/s. Wu et al. have demonstrated that the optimal chitosan concentration for production of chitosan scaffold was around 8% due to rheological properties of chitosan. Gelation process can be achieved via neutralization in NaOH (Bergonzi et al., 2019) or KOH (Liu et al., 2018) but also by Na_2CO_3 , ammonia vapours or by freeze gelation.

Some studies, shown the possibility to make composites with chitosan in association of other polymers or bioplastics to reinforce their properties or their mechanical resistance. A brief summary, of some of the most important chitosan-based composites is presented at Table 24. Some of them have never been used yet in 3D printing processes.

For instance, for the preparation of PLA-g-MA/CS composites chitosan is dried several times at 50°C and mixed with PLA grafted maleic acid (PLA-g-MA) at 180°C until melting, then the mixture is slowly extruded and cooled to obtain 3D printed strips- (Tanase and Spiridon, 2014). Various mass ratio could be used from 5/95 to 20/80 (chitosan/PLA-g-MA). Better mechanical and antimicrobial properties were found for 20/80 mass ratio. PLA grafted maleic acid allow a better compatibility with CS (Correlo et al., 2005).

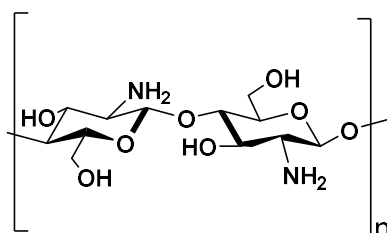


Fig. 24 Structure of chitosan

Table 24 Main green chitosan composites for potential applications in 3D printing

References	Composites	Manufacturing method
Ng, 2016	Chitosan/gelatine	3D printing
Thuaksuban et al., 2001	PCL/chitosan	Melt stretching and multilayer deposition
Tanase and Spiridon, 2014	PLA/chitosan/keratin	Blending and pressing
Wu, 2016	PLA-g-MA/Chitosan	Blending, extrusion and 3D printing
Nishant et al., 2018	PVC/PP/HAp/chitosan	FDM, 3D printing

For medical applications, chitosan can be also blended with PCL (Thuaksuban et al., 2001). In this case, chitosan microparticles were mixed with PCL but immiscibility of PCL and CS was observed. It is the same behaviour with PBS, PBAT and PBSA (Harris et al., 2019) [155]. PCL-20%CS blend obtained optimum results in term of physical properties. Chitosan could also be blended with hydroxyapatite and biocompatible plastics such as PVC, PP to reinforce physical properties of 3D printed scaffolds (Nishant et al, 2018). As a conclusion, chitosan is a promising polymer for production of biocompatible and biodegradable green materials with enhanced mechanical properties and strong biological activities.

4 Conclusion

3D printing has well earned its place in the fabrication of green material using green polymers and is probably at the first steps of its industrial development. However even if this technology is currently becoming an industrial tool in the field of synthetic materials (or metallic material for additive manufacturing) its use remains very limited applied to green polymers for the construction of 3D bio-based and/or biodegradable materials despite the abundance in nature of biopolymers and the progress of the green chemistry applied to polymers. This observation can be explained as the majority of low costs biopolymers such as polysaccharides have low printing performances. Moreover, other non-natural green polymers with better printing ability have often a cost too high for material applications even in the 3D printing area. The formulation of biopolymers as chemically modified biopolymers or their use in combination with other polymers obtained from green chemistry (polycaprolactone for example) having better printing properties could be the first step of future developments. In parallel, the increase in performance of new generation of 3D printers will probably open the way to the gradual utilization of biopolymers. The requirements of the regenerative medicine for patient specific prosthetic devices, biocompatible hydrogels and dried scaffolds with high levels of biocompatibility and/or biodegradability will be probably the greatest opportunity for increase the market share of green polymers. If this field of application could constitute an opportunity in a near future

for 3D printing applied to green polymers, the contribution of 3D printing and green polymers to the urgent and necessary eco-industrial revolution of the 21st century appears as evident on longer terms. Indeed, in 2050, 9 billion of people will be living on earth consuming considerable amounts of raw materials. Many of these resources and notably fossil fuel and metals are not infinitely available and limited. In contrast, biosourced raw materials including the major part of green polymers are renewable and can fulfill the needs of next generations if we succeed to change for a bio-based economy. In this economy the promise of 3D printing with green polymers is mainly its ability to create a sustainable and circular manufacturing process to manufacture goods locally when people need them. For that, 3D printing have to use renewable bioresources such as green polymers but also renewable energies and not fossil ones, the development of 3D printing, green polymers and renewable energy going hand in hand.

References

- Abdelwahab M., Flynn A., Chiou B-S, Imam S., Orts W., Chiellini E., 2012, Thermal, mechanical and morphological characterization of plasticized PLA-PHB blends, *Polymer Degradation and Stability* 97, 1822-1828, DOI: 10.1016/j.polymdegradstab.2012.05.036
- Albertsson A.C., Karlsson S., 1996, Controlled degradation by artificial and biological processes, *Macromolecular Design of Polymeric Materials*, Marcel Dekker, p. 54.
- Anderson S., Zhang J., Wolcott M., 2013, Effect of interfacial modifiers on mechanical and physical properties of the PHB composite with high wood flour content, *Journal of Polymer Environment* 21, 631-639; DOI: 10.1007/s10924-013-0586-y
- Armentano I., Fortunati E., Burgos N., Dominici F., Luzi E., Fiori S., Jiménez A., Yoon K., Ahn J., Kang S., Kenny J.M., 2015, Processing and characterization of plasticized PLA/PHB blends for biodegradable multiphase systems, *eXPRESS Polymer Letters* 9, 583-596, DOI: 10.3144/expresspolymlett.2015.55
- Auras R., Harte B., Selke S., 2004, An overview of polylactides as packaging materials, *Macromolecular Biosciences*, 4, 835-864, DOI: 10.1002/mabi.200400043
- Avella M., Martuscelli E., Raimo M., 2000, Review: properties of blends and composites based on poly(3-hydroxybutyrate (PHB) and poly(3-hydroxybutyrate-hydroxyvalerate) (PHBV) copolymers, *Journal of materials science* 35, 523-545, DOI: 10.1023/A:1004740522751
- Avérous L., 2004, Biodegradable multiphase systems based on plasticized starch: a review, *Journal of Macromolecular Science - Polymer Reviews*, 44, 231-274, DOI: 10.1081/MC-200029326
- Avérous L., Halley P. J., 2009, Biocomposites based on plasticized starch, *Biofuels, Bioproducts and Biorefining*, 3, 329-343, DOI: 10.1002/bbb.135
- Avérous L., Moro L., Dole P., Fringant C., 2000, Properties of thermoplastic blends : starch-polycaprolactone, *Polymer* 41, 4157-4167, DOI:10.1016/S0032-3861(99)00636-9
- Bai Y., Jiang C., Wang Q., Wang T., 2013, A novel high mechanical strength shape memory polymer based on ethyl cellulose and polycaprolactone, *Carbohydrate Polymers*, 96, 522-527, DOI: 10.1016/j.carbpol.2013.04.026
- Bai Z., Shi K., Su T., Wang Z., 2018, Correlation between the chemical structure and enzymatic hydrolysis of poly(butylene succinate), poly(butylene adipate) and

- poly(butylene suberate), *Polymer Degradation and Stability*, 158, 111-118, DOI: 10.1016/j.polymdegradstab.2018.10.024
- Balogová A., Hudák R., Tóth T., Schnitzer M., Feranc J., Bakoš D., Živčák J., 2018, Determination of geometrical and viscoelastic properties of PLA/PHB samples made by additive manufacturing for urethral substitution, *Journal of biotechnology* 284, 123-130 DOI: 10.1016/j.jbiotec.2018.08.019
- Beltran F., Infante C., Ulagares de la Orden M., Martinez Urreaga J., 2019, Mechanical recycling of poly(lactic acid): Evaluation of a chain extender and a peroxide as additives for upgrading the recycled plastic, *Journal of cleaner Production* 219, 46-56, DOI: 10.1016/j.jclepro.2019.01.206
- Bergonzi C., Di Natale A., Zimetti F., Marchi C., Biznchera A., Bernini F., Silvestri M., Bettini R., Elviri L., 2019, Study of 3D-Printed Chitosan Scaffold Features after Different Post-Printing Gelation Processes, *Scientific Reports* 9, 362, DOI:10.1038/s41598-018-36613-8
- Bossard C.D., Granel H., Jallot E.D., Vial C., Tiainen H., Wittrant Y., Lao J., 2018, Polycaprolactone / bioactive glass hybrid scaffolds for bone regeneration, *bglass* 4(1), 108-122, DOI: 10.1515/bglass-2018-0010
- Brasselet C., Pierre G., Dubessay P., Dols-Lafargue M., Coulon J., Maupeu J., Vallet-Courbin A., de Baynast H., Doco T., Michaud P., Delattre C., 2019, Modification of Chitosan for the Generation of Functional Derivatives, *Applied Sciences* 9, 1321-1354, DOI: 10.3390/app9071321
- Brüster B., Addiego F., Hassouna F., Ruch D., Raquez J., Dubois P., 2016, Thermomechanical degradation of plasticized poly(lactide) after multiple reprocessing to simulate recycling: multi-scale analysis and underlying mechanisms. *Polymer Degradation and Stability*. 131, 132-144, DOI:10.1016/j.polymdegradstab.2016.07.017
- Castles F., Isakov D., Lui A., Lei Q., Dancer C.E.J., Wang Y., Janurudin J.M., Speller S.C., Grovenor C.R. M., Grant P.S., 2016, Microwave dielectric characterisation of 3D-printed BaTiO₃/ABS polymer composites, *Scientific Reports*, vol. 6, #22714. DOI:10.1038/srep22714
- Chandra R., Rustgi R., 1998, Biodegradable polymers, *Prog. Polym. Sci.* 23(7), 1273-1335, DOI: 10.1016/S0079-6700(97)00039-7
- Chen B., Sun K., 2005, Mechanical and dynamic viscoelastic properties of hydroxyapatite reinforced poly(ϵ -caprolactone), *Polym. Test.* 24(8), 978-982, DOI: 10.1016/j.polymertesting.2005.07.013
- Chen H., Xie F., Chen L., Zheng B., 2019, Effect of rheological properties of potato, rice and corn starches on their hot-extrusion 3D printing behaviors, *Journal of Food Engineering* 244, 150-158, DOI: 10.1016/j.jfoodeng.2018.09.011
- Chiulan I., Frone A, Brandabur C., Panaitescu D., 2018, Recent advances in 3D printing of aliphatic polyesters, *Bioengineering* 5, 2, doi: 10.3390/bioengineering5010002
- Chun Y., Kyung Y. J., Jung H. C., Kim W. N., 2000, Thermal and rheological properties of polycaprolactone and polystyrene blends, *Polymer* 41, 8729-8733, DOI:10.1016/S0032-3861(00)00263-9
- Copper-White J.J., Mackay M.E., 1999, Theological properties of poly(lactides). Effect of molecular weight and temperature on the viscoelasticity of poly(L-lactic acid). *Journal of Polymer Science Part B: 37*, 1803-1814, DOI:10.1002/(SICI)1099-0488(19990801)37:15<1803::AID-POLB5>3.0.CO;2-M
- Correa D., Papadopoulou A., Guberan C., Jhaveri N., Reichert S., Menges A., Tibbits S., 2015, 3D-Printed Wood: Programming Hygroscopic Material Transformations, *3D Printing and additive manufacturing*, 2, 106-116, DOI:10.1089/3dp.2015.0022

- Correlo V.M., Boesel L., Bhattacharya M., Mano JF, Neves NM, Reis R., 2005, Properties of melt processed chitosan and aliphatic polyester blends, *Mater. Sci. Eng. A* 403, 57-68, DOI:10.1016/j.msea.2005.04.055
- Dai L., Cheng T., Duan C., Zhao W., Zhang W., Zou X., Aspler J., 2019, 3D printing using plant-derived cellulose and its derivatives : a review, *Carbohydrate Polymers* 203, 71-86, DOI: 10.1016/j.carbpol.2018.09.027
- Daver F., Marciand Lee K., Brandt M., Shanks R., 2018, Cork-PLA composite filaments for fused deposition modeling, *Composites Science and Technology* 168, 230-237, DOI: 10.1016/j.compscitech.2018.10.008
- Davidson J., Appuhamillage G., Thompson C., Voit W., 2018, Design Paradigm Utilizing Reversible Diels–Alder Reactions to Enhance the Mechanical Properties of 3D Printed Materials, *Applied Materials and Interfaces* 8, 16961-16966, DOI: 10.1021/acsami.6b05118
- de Franca da Silva Freitas D., Cestari S. P., Mendes L. C.. 2017, Natural and synthetic fillers for reaching high performance and sustainable hybrid polymer composites (chapter 7), p. 157-171, in V.K. Thakur, M.K. Thakur, R.K. Guopta. *Hybrid Polymer Composite Materials*, Woodhead Publishing, 390 p, DOI: 10.1016/B978-0-08-100789-1.00007-1
- Domínguez-Robles J., Martin N.K., Fong M.L., Stewart S.A., Irwin N.J., Rial-Hermida M.I., Donnelly R.F., Larrañeta E., 2019, Antioxidant PLA composites containing lignin for 3D printing applications: a potential material for healthcare applications. *Pharmaceutics* 11, 165, DOI: 10.3390/pharmaceutics11040165
- Dorgan J., Janzen J., Clayton M., Hait S., Knauss D., 2005, Melt rheology of variable L-content poly(lactic acid), *Journal of Rheology*, 49, 607-619, DOI: 10.1122/1.1896957
- Dorgan J., Lerhermeier H., Mang M., 2000, Thermal and Rheological properties of commercial grade poly(lacti acid)s , *Journal of polymers and the environment* vol 8, 1-9, DOI:10.1023/A:1010185910301
- Engelberg I., Kohn J., 1991, Physico-mechanical properties of degradable polymers used in medical applications: A comparative study, *Biomaterials* 12(3), 292-304, doi:10.1016/0142-9612(91)90037-b
- Fang Q., Hanna M. A., 1999, Rheological properties of amorphous and semicrystalline poly lactic acid polymers, *Industrial Crops and Products* 10, 47-53, DOI: 10.1016/S0926-6690(99)00009-6
- Garlotta D., 2001, A Literature review of Poly(Lactic Acid), *Journal of Polymers and the Environnement*, 9, 63-84, DOI: 10.1023/A:1020200822435
- Ghanbari A., Tabarsan T., Ashori A., Shakeri A., Mashkour M., 2018, Preparation and characterization of thermoplastic starch and cellulose nanofibers as green nanocomposites: Extrusion processing, *International Journal of Biological Macromolecules* 112, 442-447 , DOI: 10.1016/j.ijbiomac.2018.02.007
- Gkartzou E., Koumoulos E.P., Charitidis C. A., 2017, Production and 3D printing processing of bio-based thermoplastic filament. *Manufacturing Rev.* 4, DOI: 10.1051/mfreview/2016020
- Gómez-Lizárraga K.K., Flores-Morales C., Del Prado-Audelo M.L., Álvarez-Pérez M.A., Piña-Barba M.C., Escobedo C., 2017, Polycaprolactone- and polycaprolactone/ceramic-based 3D-bioplotted porous scaffolds for bone regeneration: A comparative study, *Mater. Sci. Eng., C* 79, 326-335, DOI: 10.1016/j.msec.2017.05.003.
- Graessley. W.W.,1967, Viscosity of Entangling Polydisperse Polymers, *J. Chem. Phys.* 47(6), 1942-1953, DOI: 10.1063/1.1712222

- Gross R.A., Kalra B., 2002, Biodegradable Polymers for the Environment, *Science* 297(5582), 803, DOI:10.1126/science.297.5582.803
- Grosvenor M.P., Staniforth J.N., 1996, The effect of molecular weight on the rheological and tensile properties of poly(ϵ -caprolactone), *Int. J. Pharm.* 135(1), 103-109, DOI: 10.1016/0378-5173(95)04404-3
- Gupta A.P., Kumar V., 2007, New emerging trends un synthetic biodegradable polymers – Polylactide: a critic, *European Polymer Journal*, 43, 4053-4074, DOI:10.1016/j.eurpolymj.2007.06.045
- Hamad K., Kaseem M., Yang H.W., Deri F., Ko Y. G., 2015, Properties and medical applications of polylactic acid:A review, *eXPRESS Polymer Letters* Vol.9, No.5, 435–455, DOI: 10.3144/expresspolymlett.2015.42
- Harris M., Potgieter J., Archer R., Arif K.M., 2019, Effect of Material and Process Specific Factors on the Strength of Printed Parts in Fused Filament Fabrication: A Review of Recent Developments, *Materials (Basel)* 12(10). pii: E1664, DOI: 10.3390/ma12101664
- Hendriks S., Kascholke C., Flath T., Schumann D., Gressenbuch M., Schulze F.P., . . . Schulz-Siegmund M, 2016, Indirect rapid prototyping of sol-gel hybrid glass scaffolds for bone regeneration – Effects of organic crosslinker valence, content and molecular weight on mechanical properties, *Acta Biomater.* 35, 318-329, DOI: 10.1016/j.actbio.2016.02.038
- Hopmann C., Schippers S., Höfs C, 2015, Influence of recycling of poly(lactic acid) on packaging relevant properties. *Journal of Applied Polymer Science* 132, 41532, DOI: 10.1002/app.41532
- Hu J., Zhu Y., Huang H., Lu J., 2012, Recent advances in shape-memory polymers: Structure, mechanism, functionality, modeling and applications. *Progress in Polymer Science*, 37, 1720-1763. DOI: 10.1016/j.progpolymsci.2012.06.001
- Hull C. W., 1986, Apparatus for production of three-dimensional objects by stereolithography, USA patent no. 4,575,330, 16 p
- Jambeck J.R., Geyer R., Wilcox C., Siegler, T.R., Perryman M., Andrady A., Narayan R., Lavender Law K., 2015, Plastic waste inputs from land into the ocean, *Science*, 347, 768-771, DOI: 10.1126/science.1260352
- Jamshidi K., Hyon S.H., Ikada Y., 1988, Thermal characterization of polylactides, *Polymer* 29, 2229-2237, DOI: 10.1016/0032-3861(88)90116-4
- Jamshidian M., Arab Tehrany E., Imran M., Jacquot M., Desobry S., 2010, Poly-Lactic acid: Production, applications, nanocomposites and release studies, *Comprehensive Reviews in Food Science and food safety* 3, 552-571, DOI: 10.1111/j.1541-4337.2010.00126.x
- Joshi P., Madras G., 2008, Degradation of polycaprolactone in supercritical fluids, *Polym. Degrad. Stab.* 93(10), 1901-1908, DOI: 10.1016/j.polymdegradstab.2008.07.002
- Kalambur S., Rizvi S., 2006, on overview of starch-based plastic blends from reactive extrusion, *Journal of plastic film and sheeting*, 22, 39-58 , DOI: 10.1177/8756087906062729
- Kariz M., Sernka M., Obućinab M., Kitek Kuzma M., 2018, Effect of wood content in FDM filament on properties of 3D printed parts, *Materials Today Communications* 14, 13, DOI: 10.1016/j.mtcomm.2017.12.016.
- Kaya M., Lelešius E., Nagrockaitė R., Sargin I., Arslan G., Mol A., Baran T., Can E., Bitim B., 2015, Differentiations of Chitin Content and Surface Morphologies of Chitins Extracted from Male and Female Grasshoper Species, *PloS One* 10(1), e0115531, DOI: 10.1371/journal.pone.0115531

- Keetels C., Van Vliet T., Walstrat P., 1996, Gelation and retrogradation of concentrated starch systems : 1 Gelation, *Food Hydrocolloids* 10, 343-353, DOI: 10.1016/S0268-005X(96)80011-7
- Khatri B., Lappe K., Noetzel D., Pursche K., Hanemann T., 2018, A 3D-Printable Polymer-Metal Soft-Magnetic Functional Composite, *Development and Characterization*, 11, #189. DOI: 10.3390/ma11020189
- Kodama H., 1981, Automatic method for fabricating a three-dimensional plastic model with photo-hardening polymer. *Rev. Sci. Instrum.*, 1770-1773, DOI: 10.1063/1.1136492
- Kopinke F.D., Remmler M., Mackenzie K., Möder M., Wachsen O., 1996, Thermal decomposition of biodegradable polyesters - II. Poly(lactic acid), *Polymer Degradation and Stability*, 1996, 53(3):329-342, DOI: 10.1016/0141-3910(96)00102-4
- Kosik-Kozioł A., Graham E., Jaroszewicz J., Chlanda A., Kumar P.T.S., Ivanovski S., . . . Vaquette C., 2019, Surface Modification of 3D Printed Polycaprolactone Constructs via a Solvent Treatment: Impact on Physical and Osteogenic Properties, *ACS Biomater. Sci. Eng.* 5(1), 318-328, DOI: 10.1021/acsbiomaterials.8b01018
- Koyama N., Doi Y., 1997, Miscibility of binary blends of poly[(R)-3-hydroxybutyric acid] and poly[(S)-lactic acid]. *Polymer* 38, 1589-1593, DOI:10.1016/S0032-3861(96)00685-4
- Kumagai T., Doi Y., 1992, Enzymatic morphologies of binary blends microbial poly(3-hydroxybutyrate) with poly(ϵ -caprolactone), poly(1,4-butylene adipate and poly(vinylacetate) , *Polymer Degradation and Stability*, 36, 241-248, DOI: 10.1016/0141-3910(92)90062-A
- Labet M., Thielemans W., 2009, Synthesis of polycaprolactone: a review, *Chem. Soc. Rev.* 38(12), 3484-3504, DOI: 10.1039/b820162p
- Lam C.X.F., S.H. Teoh, Hutmacher D.W., 2007, Comparison of the degradation of polycaprolactone and polycaprolactone-(β -tricalcium phosphate) scaffolds in alkaline medium, *Polym. Int.* 56(6), 718-728, DOI: 10.1002/pi.2195
- Le Duigou, A., Castro M., Bevan R., Martin N., 2016, 3D printing of wood fibre biocomposites: From mechanical to actuation functionality, *Materials and Design*, 96, 106–11, DOI: 10.1016/j.matdes.2016.02.018
- Leitsch H. J., 1936. Soldering iron, USA patent no. 2,054,506, 3 p.
- Lepoittevin B., Devalckenaere M., Pantoustier N., Alexandre M., Kubies D., Calberg C., . . . Dubois P., 2002, Polycaprolactone/clay nanocomposites prepared by melt intercalation: Mechanical, thermal and rheological properties, *Polymer* 43, 4017-4023 DOI: 10.1016/S0032-3861(02)00229-X
- Li T., Aspler J.S., Frascini C., Kousini L., Zhang Y., Cormier L., 2019 Lignin-containing filaments for fused deposition modelling 3D printing, in: FPIPRODUCT-173-1399, Accessed June 2019, <https://fpinnovations.ca/Extranet/Pages/AssetDetails.aspx?item=/Extranet/Assets/ResearchReportsPPB/PRR2000.pdf#>
- Lim L., Auras R., Rubino M., 2008, Processing technologies for poly(lactic acid), *progress in Polymer Science* 33, 820-852, DOI: 10.1016/j.progpolymsci.2008.05.004
- Liu Q., Li Q., Xu S., Zheng Q., Cao X., 2018, Preparation and Properties of 3D Printed Alginate-Chitosan Polyion Complex Hydrogels for Tissue Engineering, *Polymers* 10(6), 664 , DOI: 10.3390/polym1006066
- Liu J., Sun L., Xu W., Wang Q., Yu S., Sun J., 2019,, Current advances and future perspectives of 3D printing natural derived biopolymers, *Carbohydrate Polymers* 207, 297-316, DOI: 10.1016/j.carbpol.2018.11.077

- Madhavan Nampoothiri K., Rajendran Nair N., Pappy John R., 2010, An overview of the recent developments in polylactide (PLA) research, *Bioresource Technology* 101, 8493-8501, DOI: 10.1016/j.biortech.2010.05.092.
- Más Estellés J., Vidaurre A., Meseguer Dueñas J.M., Castilla Cortázar I., 2008, Physical characterization of polycaprolactone scaffolds, *J. Mater. Sci.: Mater. Med.* 19(1), 189-195, DOI: 10.1007/s10856-006-0101-2
- Menčík P., Přikryl R., Stehnová I., Melčová V., Kontárová S., Figalla S., Alexy P., Bočkaj J., 2018, Effect of Selected Commercial Plasticizers on Mechanical, Thermal, and Morphological Properties of Poly(3-hydroxybutyrate)/Poly(lactic acid)/Plasticizer Biodegradable Blends for Three-Dimensional (3D) Print, *Materials* 11, 1893, DOI: 10.3390/ma11101893
- Mittal V., Akhtar T., Matsko N., 2015, Mechanical, Thermal, Rheological and Morphological Properties of Binary and Ternary Blends of PLA, TPS and PCL, *Macromol. Mater. Eng.* 300(4), 423-435, DOI: 10.1002/mame.201400332
- Mitrus M., 2009, TPS and Its Nature. In: Leon Janssen, Moscicki L, editors. *Thermoplastic Starch A Green Material for Various Industries*. Weinheim: Wiley-VCH Verlag GmbH & Co. KGaA; . p. 77-104
- Murphy C. A., Collins M.N., 2016, Microcrystalline cellulose reinforced polylactic acid biocomposite filaments for 3D printing, *Polymer composites* 39, 1311-1320, DOI: 10.1002/pc.24069
- Nägele H., Pfitzer J., Nägele E., Inone E. R., Eisenreich N., Eckl W., Eyerer P., 2002, Arboform® - A Thermoplastic, Processable Material from Lignin and Natural Fibers, in *Chemical Modification, Properties, and Usage of Lignin*, ed. by T. Q. Hu (Springer, New-York, 2002), pp. 101-119, DOI:10.1007/978-1-4615-0643-0_6
- Nedelcu D., Ciofu C., Lohan N.M., 2013, Microindentation and differential scanning calorimetry of "liquid wood". *Composites: Part B* 55, 11-15, DOI: 10.1016/j.compositesb.2013.05.024
- Neufurth M., Wang X., Wang S., Steffen R., Ackermann M., Haep N.D., . . . Müller W.E.G., 2017, 3D printing of hybrid biomaterials for bone tissue engineering: Calcium-polyphosphate microparticles encapsulated by polycaprolactone, *Acta Biomater.* 64, 377-388, DOI: 10.1016/j.actbio.2017.09.031
- Nessi V., Rolland-Sabaté A, Lourdin D., Jamme F., Chevifny C., Kansou K., 2018, Multi-scale characterization of thermoplastic starch structure using Second Harmonic Generation imaging and NMR, *Carbohydrate Polymers* 194, 80-88, DOI: 10.1016/j.carbpol.2018.04.030.
- Nishant R., Rupinder S., Inderpreet A.,S., 2018, Biocompatible Thermoplastic Composite Blended With HAp and CS for 3D Printing in Reference Module in Materials Science and Materials Engineering, Elsevier, 1-9, DOI: 10.1016/B978-0-12-803581-8.11237-8
- Ng W.L., Yeong W.Y, Naing M.W., 2016, Polyelectrolyte gelatin-chitosan hydrogel optimized for 3D bioprinting in skin tissue engineering, *International Journal of Bioprinting* 2(1), 53-62, DOI:10.18063/IJB.2016.01.009
- Nguyen N.A., Meek K.M., Bowland C.C., Barnes S.H., Naskar A.K., 2017, Anacrylonitrile-butadiene-lignin renewable skin with programmable and switchable electrical conductivity for stress/strain-sensing applications, *Macromolecules*, DOI: 10.1021/acs.macromol.7b02336
- Nguyen N.A., Barnes S.H., Bowland C.C., Meek K.M., Littrell K.C., Keum J.K., Naskar A.K., 2018a, A path for lignin valorization via additive manufacturing of high-performance

- sustainable composites with enhanced 3D printability. *Sci. Adv.* 4, DOI: 10.1126/sciadv.aat4967
- Nguyen N.A., Bowland C.C., Naskar A.K., 2018b, A general method to improve 3D-printability and inter-layer adhesion in lignin-based composites. *Applied Materials Today* 12, 138–152, DOI: 10.1016/j.apmt.2018.03.009
- Nguyen N.A., Bowland C.C., Naskar A.K., 2018c, Mechanical, thermal, morphological, and rheological characteristics of high performance 3D-printing lignin-based composites for additive manufacturing applications. *Data in Brief* 19, 936–950 DOI: 10.1016/j.apmt.2018.03.009
- Nguyen N.A., Bowland C., Keum J.K., Staub A.X., Kearney L.T., Long J.L, Naskar A.K., 2019, Confinement and alignment of miscible amorphous lignin in polypropylene and polyethylene by 3D-printing and melt-spinning, in: *American Chemical Society Washington, D. C, Abstracts of Papers, 257th ACS National Meeting & Exposition, Orlando, FL, United States*
- Obielodan J., Helman J., Grumbles A., 2018, Development of a Thermoplastic Biocomposite for 3D Printing, in: *Proceedings of the 29th Annual International Solid Freeform Fabrication Symposium – An Additive Manufacturing Conference*
- Okada M., 2002, Chemical syntheses of biodegradable polymers, *Prog. Polym. Sci.* 27(1), 87–133, DOI: 10.1016/S0079-6700(01)00039-9.
- Oksman K., Aitomäki Y., Mathew A.P., Siqueira G., Zhou Q., Butylina S., Tanpichai S., Zhou X., Hooshmand S., 2016, Review of the recent developments in cellulose nanocomposite processing. *Composites Part A Appl Sci Manuf* 83:2–18, DOI: 10.1016/j.compositesa.2015.10.041
- Ou-Yang Q., Guo B., Xu J., 2018, Preparation and characterization of poly(butylene succinate)/polylactide blends for fused deposition modeling 3D printing, *ACS Omega* 3, 14309–14317, DOI: 10.1021/acsomega.8b02549
- Paggi R, Salmoria G., Bussolo Ghizoni G., de Madeiros Back H., de Mello Gindri I., 2019, Structure and mechanical properties of 3D-printed cellulose tablets by fused deposition modeling, *The international Journal of Advanced Manufacturing Technology* 100, 2767–2774, DOI: 10.1007/s00170-018-2830-z
- Paulsen. H C., 1965, Portable thermoplastic cement dispensers, USA patent no. 3,204,828, 3p.
- Peinado V, Castell P., Garcia L., Fernandez A., 2015, Effect of extrusion on the mechanical and theological properties of a reinforced Poly(Lactic Acid) : reprocessing and recycling of biobased materials, *Materials* 8, 7106–7117, DOI: 10.3390/ma8105360
- Peña J., Corrales T., Izquierdo-Barba I., Doadrio A.L., Vallet-Regí M., 2006, Long term degradation of poly(ϵ -caprolactone) films in biologically related fluids, *Polym. Degrad. Stab.* 91(7), 1424–1432, DOI: 10.1016/j.polymdegradstab.2005.10.016
- Peng H., G. Dai, Wang S., Xu H., 2017, The evolution behavior and dissolution mechanism of cellulose in aqueous solvent, *Journal of Molecular Liquids* 241, 959–966, DOI: 10.1016/j.molliq.2017.06.103
- Perego G., Cella G.D., Bastioli C., 1996, Effect of molecular weight and crystallinity on poly(lactic acid) mechanical properties , *Journal of Applied Polymer Science* 59, 37–43, DOI: 10.1002/(SICI)1097-4628(19960103)59:1<37::AID-APP6>3.0.CO;2-N
- Piemonte V., 2011, Bioplastic wastes: the best final disposition for energy saving. *Journal of Polymer Environment* 19, 988–994., DOI: 10.1007/s10924-011-0343-z
- Pesark J., 1938, Device for applying sealing wax, USA patent no. 2,118,415, 4p.

- Pillin I., Montrelay N., Bourmaud A., Grohens Y., 2008, Effect of thermomechanical cycles on the physico-chemical properties of poly(lactic acid). *Polymer Degradation and Stabilization* 93, 321-328, DOI: 10.1016/j.polymdegradstab.2007.12.005.
- Rudnik, E., 2013, Compostable polymer properties and packaging applications in Plastic Film in Food packaging, *Plastics Design Library Handbook series*, 217-248, DOI: 10.1016/B978-1-4557-3112-1.00013-2
- Salin I.M., Seferis J.C., 1993, Kinetic analysis of high-resolution TGA variable heating rate data, *J. Appl. Polym. Sci.* 47(5), 847-856, DOI:10.1002/app.1993.070470512
- Scott Crump S., 1989, Apparatus and method for creating three-dimensional objects, USA patent no. 5, 121, 329, 15 p
- Shao Y., Guizani C., Grosseau P., Chaussy D., Beneventi D., 2018, Use of lignocellulosic materials and 3D printing for the development of structured monolithic carbon materials. *Composites Part B* 149, 206–215, DOI: 10.1016/j.compositesb.2018.05.035
- Shibata M., Takachiyo K-I, Ozawa K., Yosomiya R., Takeishi H., 2002, Biodegradable polyester composites reinforced with short abaca fiber, *Journal of Applied Polymer Science*, 85, 129-138, DOI: 10.1002/app.10665
- Singamneni S., Smith D., Le Guen M-J., Truong D., 2018, Extrusion 3D printing of polybutyrate-adipate-terephthalate polymer composites in the pellet form, *Polymers*, 10, 922-935, DOI: 10.3390/polym10080922
- Smurthwaite Arkless R., 1951, Plastic welding device, USA patent no. 2,556,609, 3 p Hans C. Paulsen. Portable thermoplastic cement dispensers, USA patent no. 3,204,828, 3 p.
- Stephens, B. Azimi P., El Orch Z., Ramos T., 2013, Ultrafine particle emissions from desktop 3D printers, *Atmospheric Environment*, 79, 334-339, DOI: 10.1016/j.atmosenv.2013.06.050
- Sun H., Mei L., Song C., Cui X., Wang P., 2006, The in vivo degradation, absorption and excretion of PCL-based implant, *Biomaterials* 27(9), 1735-1740, DOI:10.1016/j.biomaterials.2005.09.019
- Szójka A., Lalh K., Andrews S.H.J., Jomha N.M., Osswald M., Adesida A.B., 2017, Biomimetic 3D printed scaffolds for meniscus tissue engineering, *Bioprinting* 8, 1-7, DOI: 10.1016/j.bprint.2017.08.001
- Tanase C.E., Spiridon L., 2014, PLA/chitosan/keratin composites for biomedical applications, *Mater. Sci. Eng C.* 40, 242-247, DOI: 10.1016/j.msec.2014.03.054
- Thomas S.M., DiCosimo R., Nagarajan V., 2002, Biocatalysis: applications and potentials for the chemical industry, *Trends Biotechnol.* 20(6), 238-242, DOI: 10.1016/S0167-7799(02)01935-2
- Thuaksuban N., Nuntanaranont T., Pattanachot W., Suttapreyasri S., Kwong Cheung L., 2001, Biodegradable polycaprolactone – chitosan three-dimensional scaffolds fabricated by melt stretching and multilayer deposition for bone tissue engineering ; assessment of the physical properties and cellular response, *Biomed. Mater.* 6, 015009, DOI: 10.1088/1748-6041/6/1/015009
- Ulfah I.M., Fidyansih R., Rahayu S., Fitriani D.A., Saputra D.A., Winarto D.A., Wisojodharmo L.A., 2015, Influence of Carbon Black and Silica Filler on the Rheological and Mechanical Properties of Natural Rubber Compound, *Procedia Chemistry*, 16, 258-264, DOI:10.1016/j.proche.2015.12.053
- Vaidya A., Collet C., Gaugler M., Lloyd-Jones G., 2019, Integrating softwood biorefinery lignin into polyhydroxybutyrate composites and application in 3D printing, *Materials Today Communications* 19, 286-296, DOI: 10.1016/j.mtcomm.2019.02.008

- Wang J., Wu D., Zhang Z., Li J., Shen Y., Wang Z., . . . Sun J., 2015, Biomimetically Ornamented Rapid Prototyping Fabrication of an Apatite–Collagen–Polycaprolactone Composite Construct with Nano–Micro–Macro Hierarchical Structure for Large Bone Defect Treatment, *ACS Appl. Mater. Interfaces* 7(47), 26244-26256, DOI: 10.1021/acsami.5b08534
- Wang M-J., 1998, Effect of Polymer-Filler and Filler-Filler Interactions on Dynamic Properties of Filled Vulcanizates, *Rubber Chemistry and Technology*, 71, 520-589, DOI: 10.5254/1.3538492,
- Wang Q., Sun J., Yao Q. Ji C., Liu J., Zhu Q., 2018, 3D printing with cellulose materials, *Cellulose* 25:4275–4301 , DOI: 10.1007/s10570-018-1888-y
- Wang S., Daelemans L., Fiorio R., Xia H., Zhang J., Gou M., D’Hooge D.R., de Clerck K., Cardon L., 2019, Bio-material polylactic acid poly(butylene adipate co-terephthalate) blends development for extrusion based additive manufacturing, *AUTEX 2019 – 19th World textile Conference on textiles at the Crossroads*, 11-15 June 2019, Ghent, Belgium
- Wang Z., Xu J., Lu Y., Hu L., Fan Y., Ma J., Zhou X., 2017, Preparation of 3D printable micro/nanocellulose-poly(lactic acid) (MNC/PLA) composite wire rods with high MNC constitution, *Industrial Crops and Products* 109, 889-896, DOI: 10.1016/j.indcrop.2017.09.061
- Woodruff M.A., Hutmacher D.W., 2010, The return of a forgotten polymer— Polycaprolactone in the 21st century, *Prog. Polym. Sci.* 35(10), 1217-1256, doi:10.1016/j.progpolymsci.2010.04.002, DOI: 10.1016/j.progpolymsci.2010.04.002
- Woodward S.C., Brewer P.S., Moatamed F., Schindler A., Pitt C.G., 1985, The intracellular degradation of poly(ϵ -caprolactone), *J. Biomed. Mater. Res.* 19(4), 437-444, DOI: 10.1002/jbm.820190408
- Wu C.S., 2016, Modulation, functionality, and cytocompatibility of three-dimensional printing materials made from chitosan-based polysaccharide composites, *Mater. Sci. Eng C.* 69, 27-36, doi: 10.1016/j.msec.2016.06.062
- Wu C.S., Liao H-T, 2017, Fabrication, characterization and application of polyester/wood flour composites, *Journal of Polymer Engineering*, 37, 689-698 , DOI: 10.1515/polyeng-2016-0284
- Wu C-S, Liao H-T, Cai Y-X, 2017, Characterization, biodegradability and application of palm fibre-reinforced polyhydroxyalkanoate composites, *Polymer Degradation and Stability* 140, 55-63, DOI:10.1016/j.polymdegradstab.2017.04.016
- Wu Q., Therriault D., Heuzey M-C., 2018, Processing and properties of chitosan inks for 3D printing of hydrogel microstructures, *ACS Biomater. Sci. Eng* 4, 2646-652, DOI: 10.1021/acsbiomaterials.8b00415
- Xu J., Guo B-H., 2010, Poly(butylene succinate) and its copolymers: research, development and industrialization, *Biotechnology Journal* 5, 1149-1163, DOI: 10.1002/biot.201000136
- Yang Y., Chen Y., Wei Y., Li Y., 2016, 3D printing of shape memory polymer for functional part fabrication, *The International Journal of Advanced Manufacturing Technology* 84, 2079–2095, DOI: 10.1007/s00170-015-7843-2
- Zenkiewicz M., Richert J., Rytlewski P., Moraczewski K., Stepczynska M., Karasiewicz T., 2009, Characterisation of multi-extruded poly(lactic acid). *Polymer Testing* 28, 412-418, DOI: 10.1016/j.polymertesting.2009.01.012
- Zhang M., Thomas N., 2011, Blending Poly(lactic acid) with Poly(hydroxybutyrate): The Effect on Thermal, Mechanical, and Biodegradation Properties, *Advances in Polymer Technology*, 30, 67–79, DOI: 10.1002/adv.20235

Zhao P., Liu W., Wu Q., Ren J., 2010, Preparation, Mechanical and thermal properties of biodegradable polyesters/poly(Lactic acid) blends, *Journal of Nanomaterials*, DOI: 10.1155/2010/287082

Zhao X., Hwang K.-J., Lee D., Kim T., Kim N., 2018, Enhanced mechanical properties of self-polymerized polydopamine coated recycled PLA filament used in 3D printing, *Applied Surface Science* 441, 381-387, DOI: 10.1016/j.apsusc.2018.01.257